

5-2012

## Structural Analysis of the Drosophila Innexin ShabB: Role of the N-Terminus in Rectifying Electrical Synapses

William Marks

SUNY College at Buffalo, markswd@vcu.edu

### Advisor

Dr. I. Martha Skerrett, Associate Professor of Biology

### First Reader

Dr. I. Martha Skerrett, Associate Professor of Biology

### Second Reader

Dr. Douglas P. Easton, Professor of Biology

### Third Reader

Dr. Thomas D. White, Professor of Biology

### Department Chair

Gregory J. Wadsworth, Associate Professor and Chair of Biology

To learn more about the Biology Department and its educational programs, research, and resources, go to <http://biology.buffalostate.edu/>.

---

### Recommended Citation

Marks, William, "Structural Analysis of the Drosophila Innexin ShabB: Role of the N-Terminus in Rectifying Electrical Synapses" (2012). *Biology Theses*. 2.  
[https://digitalcommons.buffalostate.edu/biology\\_theses/2](https://digitalcommons.buffalostate.edu/biology_theses/2)

Follow this and additional works at: [https://digitalcommons.buffalostate.edu/biology\\_theses](https://digitalcommons.buffalostate.edu/biology_theses)



Part of the [Biophysics Commons](#), [Molecular and Cellular Neuroscience Commons](#), and the [Molecular Biology Commons](#)

## ABSTRACT OF THESIS

Structural Analysis of the *Drosophila* Innexin ShakB:

Role of the N-Terminus in Rectifying Electrical Synapses

Gap junction channels mediate direct intercellular communication in all multicellular animals. They are comprised of the connexin family of proteins in vertebrates and the innexin family in prechordates. Connexins and innexins share many functional and structural similarities as orthologous proteins. Both types are capable of forming electrical synapses. Rectifying junctions are specialized electrical synapses found in neural systems that control escape responses. It has been shown that heterotypic gap junction channels mediate asymmetric properties of rectifying junctions. Shaking B N+16 and Shaking B lethal are variants of the ShakB locus in *Drosophila* and the organization of these innexins into heterotypic junctions underlies electrical rectification in the Giant Fiber System. The goal of this study was to further explore molecular mechanisms of rectification by establishing the role of the N-terminus. After creating a series of deletions and chimeric proteins in which the N-terminus of the innexin Shaking B Lethal was modified, proteins were characterized in paired *Xenopus* oocytes and analyzed electrophysiologically. Deletion of the N-terminus of Shaking B lethal resulted in loss of function. Replacing the N-terminus with that of Shaking B N+16 produced a chimeric protein that formed rectifying junctions when paired with wildtype, thus demonstrating that the N-terminus of innexins is crucial for channel function and plays a key role in rectification. The chimera gated symmetrically with characteristics similar to those of ShakB L, when paired homotypically, providing insight into the mechanism of voltage gating.

State University of New York  
College at Buffalo  
Department of Biology

Structural Analysis of the *Drosophila* Innexin ShalB:  
Role of the Amino-Terminus in Rectifying Electrical Synapses

A Thesis in  
Biology

by

William D. Marks

Submitted in Partial Fulfillment  
Of the Requirements  
For the Degree of

Master of Arts  
May 2012

Approved by:

I. Martha Skerrett, Ph.D.  
Associate Professor of Biology  
Chairperson of the Thesis Committee/Thesis Adviser

Gregory J. Wadsworth, Ph.D.  
Chair and Associate Professor of Biology

Kevin J. Railey, Ph.D.  
Associate Provost and Dean of the Graduate School

## Table of Contents

Abstract . . . . .	i
Title page . . . . .	ii
Table of contents . . . . .	iii
List of figures . . . . .	iv
Introduction . . . . .	1
Methods . . . . .	14
Results . . . . .	22
Discussion . . . . .	43
Works Cited . . . . .	57

## List of Figures

Figure 1: Membrane topology of connexins. ....	1
Figure 2: Hemichannel pairing nomenclature .....	2
Figure 3: Three dimensional models of connexins .....	5
Figure 4: Schematic diagram of electrical rectification in crayfish Giant Fiber System .....	7
Figure 5: Current traces demonstrating electrical rectification. ....	9
Figure 6: <i>Drosophila melanogaster</i> Giant Fiber System schematic .....	13
Figure 7: Vector maps and wildtype sequence alignments. ....	16
Figure 8: Illustrations of wildtype and mutant constructs .....	18
Figure 9: Amino acid alignment of mutant constructs .....	23
Figure 10: Example gel photograph showing DNA after linearization. ....	24
Figure 11: Example gel photograph showing RNA after <i>in vitro</i> transcription .....	24
Figure 12: Graphical comparison of junctional conductance induced by SBL-NTdel .....	26
Figure 13: Junctional currents recorded from oocytes expressing ShakB L and SBL-NTdel ..	27
Figure 14: Graphical comparison of Junctional conductance induced by SBL+N16NT-I19 ..	29
Figure 15: Junctional currents recorded from oocytes expressing ShakB L/SBL+N16NT-I19 .	30
Figure 16: Junctional currents recorded from oocytes expressing ShakB L/SBL+N16NT-I19 .	31
Figure 17: Holding voltage on gating conductance .....	32
Figure 18: Holding voltage on non-gating conductance. ....	33
Figure 19: Comparisons of junctional currents A .....	35
Figure 20: Graphical comparison of junctional conductance induced by SBL+N16NT A .....	37
Figure 21: Graphical comparison of junctional conductance induced by SBL+N16NT B .....	39
Figure 22: Junctional currents recorded from oocytes expressing ShakB L/SBL+N16NT. ...	40
Figure 23: Junctional currents recorded from oocytes expressing ShakB L/SBL+N16NT. ...	41
Figure 24: Junctional currents recorded from oocytes expressing SBL+N16NT/SBL+N16NT	42

Figure 25: Comparisons of junctional currents B .....	48
Figure 26: Comparisons of junctional currents C .....	50
Figure 27: <i>Drosophila</i> stimulation apparatus .....	54

## Introduction

### *Gap junctions*

A gap junction is a physiological feature of multicellular animals that is crucial for cell to cell communication (Laird, 2006). In vertebrates, the connexin family of proteins forms gap junctions, while prechordates utilize innexin-based gap junctions (Phelan, *et al.*, 1998b). As shown below in Figure 1, connexins are multi-pass membrane proteins with cytoplasmic carboxyl (C) and amino (N) termini as well as four transmembrane domains (M1-M4), two extracellular domains (E1/E2) and a cytoplasmic loop (CL) (Laird, 2006). Innexins share a similar structure and function with connexins, although genetically the two protein groups are not homologous (Phelan *et al.*, 1998b), and connexins are believed to have evolved convergently (Alexopoulos *et al.*, 2004).

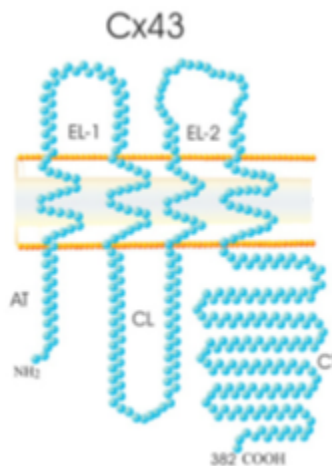


Figure 1

Figure 1. Membrane topology of connexin proteins. Gap junction proteins have four transmembrane domains (M1-M4), two extracellular domains (E1-E2), a cytoplasmic loop (CL) and amino (AT) and carboxyl (CT) termini (Laird, 2006). Reproduced with permission, from Laird, D. 2006. *Biochem. J.*, **394**, 527-543. © the Biochemical Society.

While not much is known about innexin structure and function, it is well documented that connexins oligomerize into hexamers to form connexons in adjacent cells before docking to create intercellular channels (Figure 2). Connexons are composed either of identical or non-identical connexin subunits. For example, humans express 20 different connexin proteins with overlapping expression patterns (Laird, 2006). If all six proteins comprising a connexon are identical, the connexon is homomeric, and when non-identical, the connexon is heteromeric (Laird, 2006). At sites of cell-cell communication, a connexon from one cell docks with a connexon in a neighboring cell, creating a gap junction channel. As shown in figure 2, the intact channel can be described using nomenclature similar to that used for the constituent halves. If the two hemichannels are identical, the junction is homotypic, if non-identical, the junction is heterotypic.

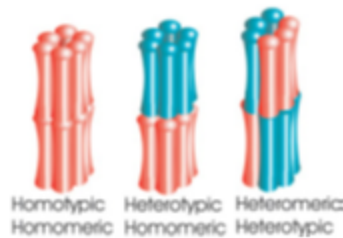


Figure 2

Figure 2. Connexin proteins form connexons, also known as hemichannels, composed of six proteins, which can be the same or different. Complete channels are formed by two hemichannels, and need not be composed of the same hemichannel type (Laird, 2006). Reproduced with permission, from Laird, D. 2006. *Biochem. J.*, **394**, 527-543. © the Biochemical Society.

It is typical that hundreds of gap junction channels cluster together in one area, creating a gap junction plaque, characterized by the close apposition of cells (Laird, 2006). It is generally assumed that connexins and innexins oligomerize similarly to form gap junction channels. Electron micrographs demonstrate that arthropod gap junctions have a similar appearance to



connexin-based junctions with a slightly wider gap than that observed in vertebrates (Leitch, 1992; Blagburn *et al.*, 1999).

Gap junctions facilitate the transport of small, biologically important molecules between cells, allowing for diffusion within tissue and direct intercellular communication (Harris, 2001). Gap junctions also play an important role in electrical coupling. Heart tissue is known to use gap junctions to transmit electrical impulses required for atrio-ventricular contraction. Electrical synapses in the nervous system of vertebrates and invertebrates, are also composed of gap junctions (Willecke *et al.*, 2002; Phelan *et al.*, 1998b.). At the site of an electrical synapse between neurons, an action potential traveling along an axon is transmitted through the gap junction into the next neuron. This allows for faster transmission than a chemical synapse and also for regulation by a wide range of physiological factors (reviewed in Bear *et al.*, 2007). Gap junction channels can exist in either an open or closed conformation, which can be altered via protein binding, phosphorylation, calcium, or voltage (In Bear *et al.*, 2007; Karp, 2008).

### *The N-terminus and junction channel physiology*

Connexins and innexins, have similar topologies despite having variations in primary structure (Phelan *et al.*, 1998b). Two extracellular loops play a role in docking of hemichannels, and three distinct cytoplasmic domains are created by a cytoplasmic loop, in addition to the C and N termini as previously shown in Figure 1. The C-terminus and cytoplasmic loops play important roles in chemical gating of connexins (Peracchia, 2004), while multiple regions including the transmembrane domains, cytoplasmic loop, and amino terminus, work together to form the voltage gating mechanism (Harris 2001).

The average connexin N-terminus chain is 20-22 amino acid residues in length (as seen in figure 1), and has a highly conserved sequence. The structure and function of the N-terminus has been studied most extensively in connexin 37 where residues 5 through 17 form an alpha helix and residues 18-22 form a flexible, helix-like structure (Kyle *et al.* 2009). Deletion of approximately half of the N-terminal residues causes the connexin to fail to localize at the cellular membrane. Smaller deletions cause loss of function without loss of membrane localization. When a series of amino acids ranging from 2 to 5 residues in length are replaced with alanine, the resultant gap junctions are not functional, suggesting that not only is the size of the chain important, but the specific sequence as well (Kyle *et al.* 2008.). Replacement of as few as two amino acids, 10 and 15 specifically, with alanine in connexin 37 causes a loss function (Kyle *et al.* 2009).

In another experiment, the N-terminus of chicken connexin 45.6 was replaced with the N-terminus of rat connexin 43. The channels composed of the chimeric proteins behaved differently than the channels composed of either connexin 45.6 or 43, however, the chimeric channels functioned more like rat connexin 43 than chicken connexin 45.6, from which most of the protein originated. The chimeric proteins behaved similarly to the protein from which the N-terminus was taken in voltage sensitivity and in selectivity based on size or charge. This further suggests that the sequence of the N-terminus plays a significant role in determining the function of the channel (Dong *et al.*, 2006).

In the crystal structure of a gap junction channel composed of connexin 26, the first thirteen residues in the N-terminus form a short helix that folds into the pore (Figure 3a; Maeda *et al.*, 2009). This is consistent with earlier electron cryocrystallography which demonstrated the presence of a plug within the pore (Figure 3b; Oshima *et al.*, 2007). Research suggests that the

plug is created when the N-termini of the constituent connexins fold into the channel as seen in the side-view of the gap junction structure after X-ray diffraction (figure 3a; Maeda *et al.*, 2009) and the top down view of the gap junction after cryo-electron microscopy (Figure 3b; Oshima *et al.*, 2007). This is consistent with studies where Cx26 mutants missing portions of the N-terminus showed a significantly decreased mass within the pore, and the channels lost functionality (Oshima *et al.*, 2008).

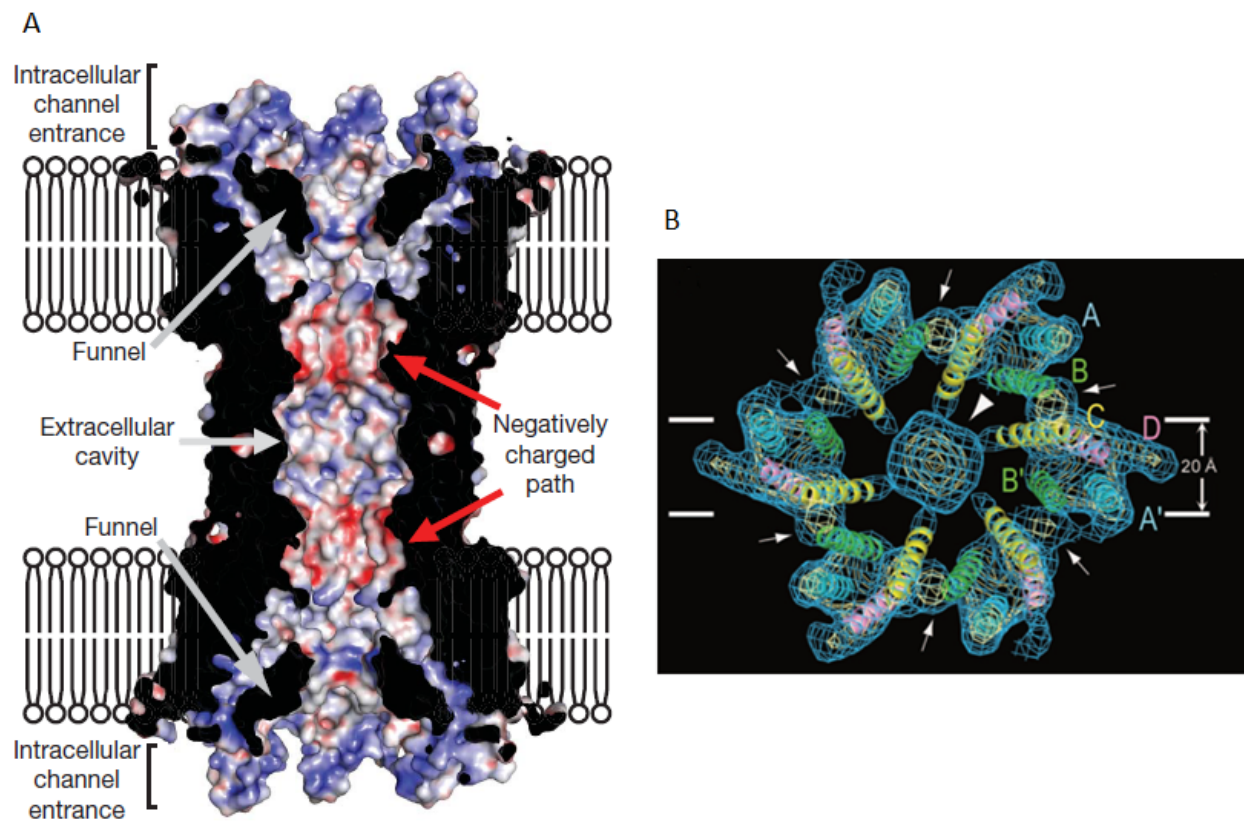


Figure 3

Figure 3. (A) Three dimensional structure after X-ray diffraction of the channel formed by connexin 26. The negatively charged path in the extracellular cavity is believed to be a site for interaction with the charged residues in the N-terminal tail (Maeda *et al.*, 2009). Reprinted with permission from Macmillan Publishers Ltd: Maeda S. Nakagawa S. Suga M. Yamashita E. Oshima A. Fujiyoshi I. Tuskihara T. Structure of the connexin 26 gap junction channel at 3.5Å resolution. Nature. 2009;458: 597-607. (c) 2009. (B) Cryo-Electron Microscopy model of a Connexin 26 hemichannel with a plug in the central pore. The view is from the extracellular surface looking down through the pore into the cell (Oshima *et al.*, 2007) Reprinted with permission from the National Academy of Sciences. Oshima, A., Tani, K., Hiroaki, Y., Fujiyoshi, I., and Sosinsky, G.E. 2007. Three-dimensional

Positioning the N-terminal chain within the pore infers interactions with residues of the pore-lining helices. Such interactions were recently identified through tryptophan-scanning analysis of Cx32 (Brennan *et al.*, *in prep.*). The results of scanning mutagenesis correlate with the crystal structure of Cx26 which identifies an interaction between W2 in the N-terminus and M34 in the first transmembrane domain, the main pore-lining domain (Maeda *et al.*, 2009). Tryptophan scanning suggests similar interactions in channels composed of Cx43 (Brennan *et al.*, *in prep.*), while interactions between the N-terminus and the first transmembrane domain were not detected in innexin-based channels (DePriest *et al.*, 2011).

### *Rectification*

Typical gap junctions are bidirectional in the sense that ions and molecules travel equally well in both directions (Karp, 2008). However, some electrical synapses favor the transmission of electrical signals in one direction, a phenomenon referred to as electrical rectification. Rectifying junctions pass current more easily in one direction than another. Generally, when the presynaptic cell is depolarized relative to the postsynaptic cell, junctional resistance is minimized. This is demonstrated in the simplified circuit diagram in Figure 4 where the presynaptic fiber is depolarized relative to the postsynaptic fiber.

Rectifying synapses have been identified in the Giant Fiber System (GFS) of crayfish (Furshpan and Potter, 1959; Jaslove and Brink, 1980) and *Drosophila* (Phelan *et al.*, 1996). In crayfish, the rectifying synapse between the giant interneuron and the motor giant axon has been well characterized using electrophysiological techniques (Jaslove and Brink, 1980). In

*Drosophila*, rectifying synapses at the junction of the giant fiber and tergotrochanteral motor neurons (TTMns) and at the junction of the Giant Fiber and the peripherally synapsing interneurons (PSIs) have been characterized using a variety of techniques (Allen *et al.*, 2006, Phelan *et al.*, 2008). Both synapses relay signals to the dorsal longitudinal muscle during the escape response, where rapid neural transmission is advantageous (Allen *et al.*, 2006).

Rectifying synapses have also been found in some chordates as well. Lampreys have a system that has a very similar neuroanatomy to the arthropod GFS, with rectifying synapses co-occurring with chemical synapses (Ringham, 1975). Hatchetfish also have a rectifying synapse that has been shown to play a role in its escape response (Auerbach & Bennett, 1969).

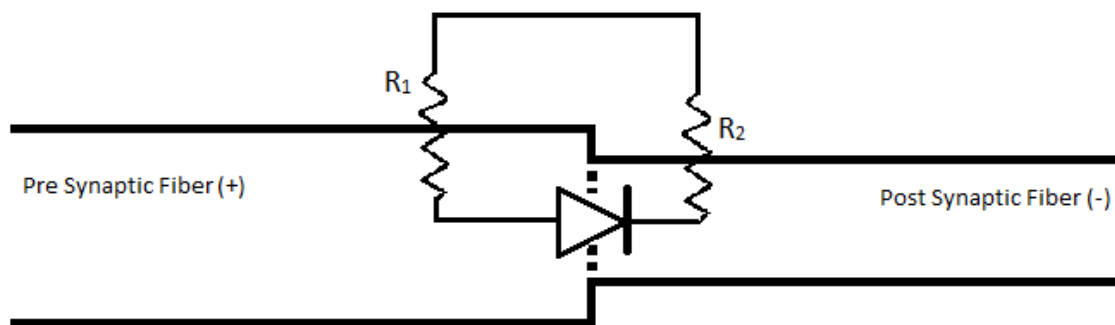


Figure 4

Figure 4. Electrical diagram showing the activity of a rectifying synapse as proposed by Furshpan and Potter (1959).  $R_1$  and  $R_2$  represent the proposed resistance of the pre- and post-synaptic membrane respectively. The electrical synapse (dashed line) is noted as a rectifier and will conduct current when the presynaptic axon is depolarized relative to the postsynaptic cell. The postsynaptic fiber is hyperpolarized prior to the junction opening, further hyperpolarization would similarly cause and increase in junctional conductance. In both cases, electrical transmission only flows in one direction. Hyperpolarizing the presynaptic axon or depolarizing the postsynaptic axon maintains that non-conductive state of the junction. Redrawn from Furshpan & Potter, 1959.

In 1959, Furshpan and Potter suggested that electrical rectification in the GFS of crayfish could be attributed to a variable resistance between two cell membranes caused by an asymmetrically structured junction. Jaslove and Brink (1980) later attributed electrical rectification to rapid and asymmetric voltage-gating of gap junction channels at the synapse. It has since been found that rectifying electrical synapses in *Drosophila* are heterotypic junctions (Phelan *et al.*, 2008). On the presynaptic side of the GF axon, Shaking B Neural+16 (ShakB N+16) is found. Postsynaptically, in either the TTMns or in the PSIs, Shaking B lethal (ShakB L) is present (Phelan *et al.*, 2008). Exogenous expression of *Drosophila* innexins in *Xenopus* allows experimental analysis of junctions composed of ShakB N+16 in one cell, and ShakB L in the other (Phelan *et al.*, 2008). This experiment demonstrated that rectifying junctions could be created through heterotypic pairing as shown in figure 5. Rectification appears to be instantaneous, meaning that current flows more easily in one direction than in another immediately upon changes in transjunctional voltage ( $V_j$ ), shown in figures 5a and 5c. As expected, junctions composed entirely of either ShakB N+16 or ShakB L showed symmetrical responses to voltage, shown in figures 5f and 5h (Phelan *et al.*, 2008).

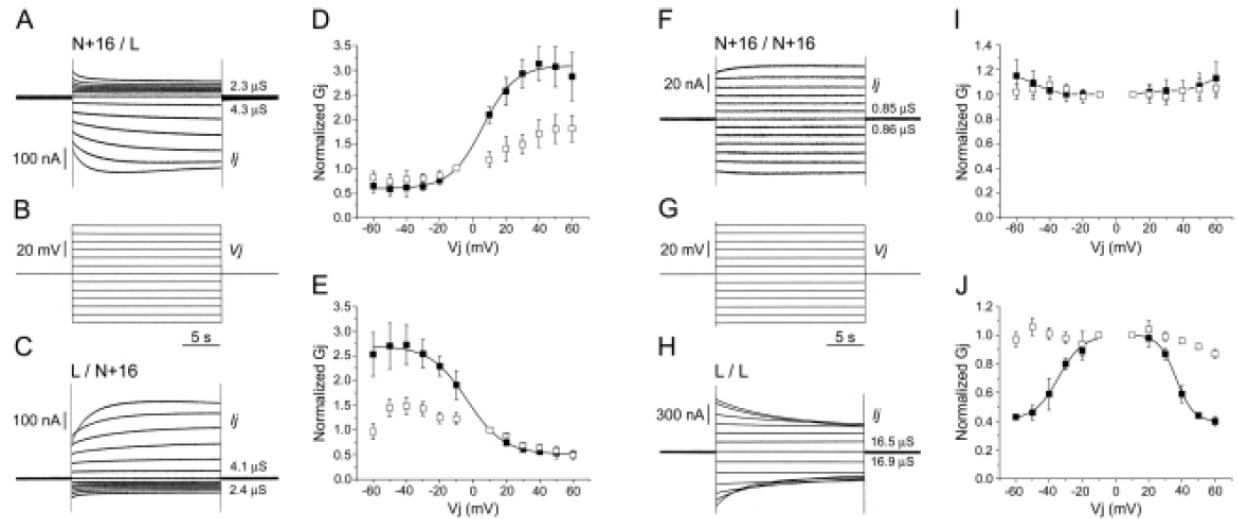


Figure 5

Figure 5. Figures 5A through 5E. Current traces and voltage sensitivity of rectifying gap junctions composed of ShakB N+16 and Shak B L. Figures 5F through 5J. Current traces and voltage sensitivity of homotypic ShakB junctions. 5A shows currents induced in *Xenopus* oocytes expressing ShakB N+16 and Shak B L, with currents recorded relative to the N+16-expressing cell. 5B is a voltage protocol trace. 5C shows currents induced in *Xenopus* oocytes expressing ShakB N+16 and Shak B L, with currents recorded relative to the L-expressing cell. 5D depicts the relationship between transjunctional voltage and junctional conductance, relative to N+16 in heterotypic pairings. The data has been fit with a Boltzman equation. Figure 5E depicts the relationship between transjunctional voltage and junctional conductance, relative to L in heterotypic pairings. The data has been fit with a Boltzman equation. 5F shows currents induced by a typical N+16 homotypic pairing and the voltage pulse protocol is shown in 5G. 5H shows currents induced by a typical L homotypic pairing. 5I depicts the relationship between transjunctional voltage and junctional conductance for N+16 homotypic pairings. The data has been fit with a Boltzman equation. 5J depicts the relationship between transjunctional voltage and junctional conductance, relative to N+16 in heterotypic pairings. The data has been fit with a Boltzman equation. (from Phelan, *et al.*, 2008). Reprinted from Curr. Biol. 18, Phelan, P., Goulding, L.A., Tam, J.L.Y., Allen, M.J., Dawber, R.J., Davies, J.A., and Bacon J.P., Molecular Mechanism of Rectification in the *Drosophila* Giant Fiber System. Pages No. 1955-1960. © (2007), With permission from Elsevier.

In connexin-based channels two types of rectification are apparent. Both have been studied at the molecular level. One form of rectification results from the pairing of hemichannels with different sensitivities to voltage (Verselis *et al.*, 1994, reviewed in Harris, 2001). The other form of rectification is known as “instantaneous” rectification. It occurs less frequently and appears to

result from asymmetry in the conduction pathway that is independent of the conformational changes associated with voltage gating (Rubin *et al.*, 1992a; Rubin *et al.*, 1992b). In the latter case rectification can result in channels that exhibit a novel response to voltage that would not be predicted by adding the voltage response of the two constituent hemichannels. A variety of factors associated with protein-protein interaction may give rise to the novel effect, including interactions between the extracellular loops of the apposed hemichannels. In studying rectification associated with heterotypic Cx32/Cx26 junctions, Rubin *et al.* (1992b) created chimeric proteins in which the E1 loop of connexin 32 was replaced with that of connexin 26. The rectification was not abolished but voltage-dependent activity was decreased, suggesting a role for E1 in rectification.

To more specifically identify the molecular components of rectification, amino acids 41 and 42 of connexin 26 were replaced with corresponding residues from connexin 32. In heterotypic pairings, a novel form of rectification was observed, different from the normal rectification response or the response of chimeric connexins (Rubin *et al.*, 1992a). In a similar study, the first and second extracellular loops and the third transmembrane domain of Cx32 were replaced with the corresponding domains of Cx26 (Rubin *et al.*, 1992b). Some degree of rectification was lost with additional changes to voltage-gating. These early studies highlight the complexity of identifying molecular components of rectification. They also highlight the complexity of identifying an instantaneous component of rectification that is independent of voltage-gating mechanisms.

Oh *et al.* (1999, 2000) studied voltage-dependent rectification in gap junction channels, a form of rectification that arises from opposite voltage gating polarity of constituent hemichannels. This type of rectification is predicted by the behavior of individual hemichannels.



Channels composed of connexin32 close in response to relatively negative voltage while channels composed of connexin26 close in response to relatively positive voltages. Heterotypic Cx32/Cx26 junctions form rectifying junctions that gate only in response to one voltage polarity. Oh *et al.* (1999) showed that changing one residue in the N terminus reversed gating polarity. Replacement of the second residue with either a charged or a neutral residue (N2D) reversed the gating polarity of Cx26 channels (Oh *et al.*, 2000). Further analysis involved the creation of chimeric proteins. The first 11 residues of the N-terminus of connexin 32, and the cytoplasmic loop of connexin 32 were replaced with the corresponding domains from connexin 26. Distinct patterns of rectification were observed for gap junctions composed of the chimeric connexin 32 paired with normal connexin 32. However, a simpler chimeric connexin 32 in which only the N-terminus was exchanged with that of Cx26 failed to display typical rectification suggesting that an interaction between the N-terminus and the cytoplasmic loop may be required for voltage-dependent rectification (Oh, *et al.* 1999).

This study is aimed at determining whether the N-terminus of ShakB N+16, contributes to the strong electrical rectification observed at heterotypic junctions composed of ShakB N+16 and ShakB L. These are the proteins known to compose the rectifying synapses in the *Drosophila melanogaster* giant fiber system (Phelan *et al.*, 2008). Interest in the N-terminus is based on studies of connexins where it has been demonstrated that charged residues in the N-terminus play a role in determining the physiological properties of the channel (Oh *et al.*, 1999). The crystal structure of a gap junction channel composed of connexin 26 shows the N-terminus drawn into the pore, interacting directly with the first transmembrane domain and contributing to the permeation path of the pore (Maeda *et al.*, 2009). It is not yet known whether innexins utilize the N-terminus in a similar way. The fact that innexins and connexins function similarly and

appear structurally similar suggests that the N terminus will play a similar role. However, innexins are most closely related to the pannexin family of proteins and it has recently been demonstrated that conduction pathway of pannexins is complex and likely to involve contributions for the C-terminus (Wang & Dahl, 2010). The work performed in this study, involving chimeras of Shaking B proteins, demonstrates an important role of the N-terminus in heterotypic junction channels composed of innexins.

### *The Drosophila melanogaster Giant Fiber System*

The rectifying junction of ShakB L and ShakB N+16 *in vivo* is found in the Giant Fiber System of the fruit fly, which mediates the escape responses involved in simultaneous jumping and flight (Allen *et al.*, 2006; Phelan *et al.*, 2008). As noted in figure 6, two neurons originate in the brain, run along the ventral nerve cord, and fork out at the second pair of legs. These are the Giant Fibers. In the “brain region”, the two Giant Fibers are linked by the Giant Commissural Interneurons (GCIs). At the fork, a large synaptic region is found between the GFs and the TTMns. The TTMns innervate the tergotrochanteral muscle, which is responsible for the jumping portion of the escape response. Just prior to the fork, the GFs also synapse with the PSIs. The PSIs then synapse electrically with the Dorsal Longitudinal Motor neurons (DLMns), which innervate the Dorsal Longitudinal muscles which cause the wings to flap. Rectifying synapses are found between the GFs and the TTMns, and between the GFs and the PSIs, and are noted with arrows in figure 6 (Allen *et al.*, 2006). Electrical synapses found in the brain region, and between the PSIs and DLMns are not rectifiers, but are composed of ShakB N+16, with a small number of junctions composed of Shaking B Neural (Phelan *et al.*, 2008). Both rectifying

synapses are localized in a mixed synaptic region, containing both electrical synapses and chemical synapses (Allen *et al.* 2006).

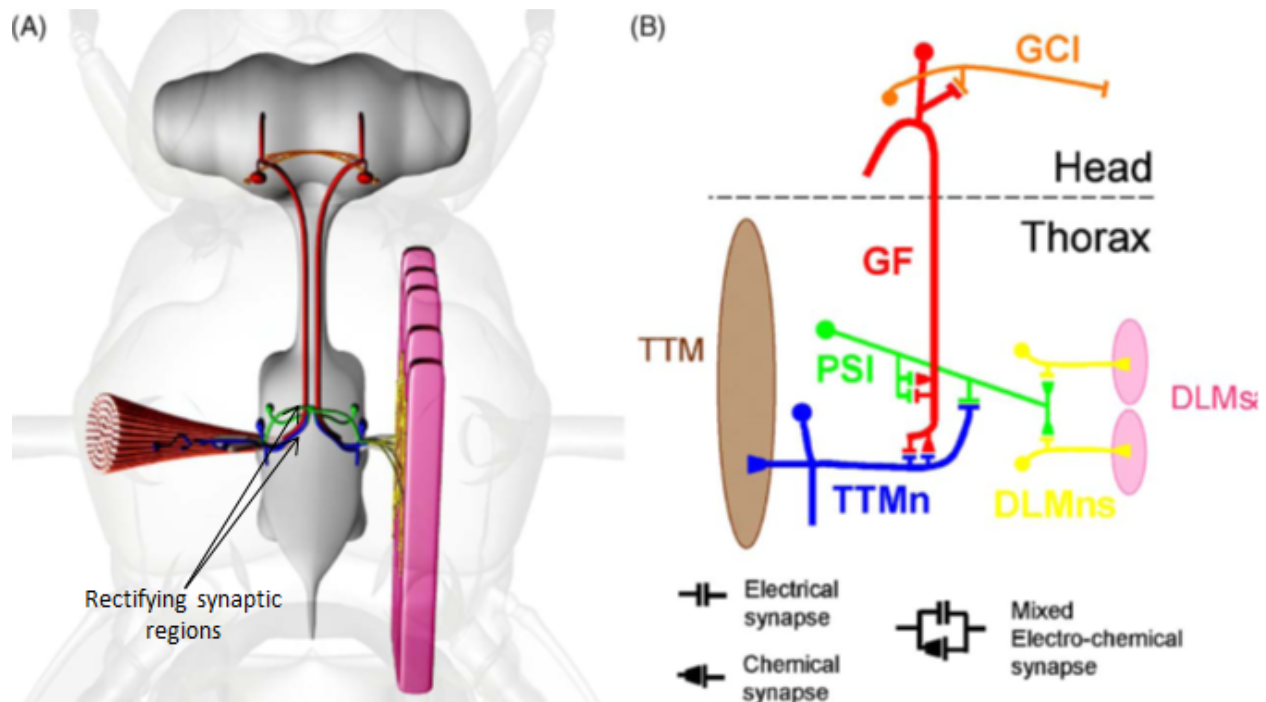


Figure 6

Figure 6. (A) Three dimensional rendering of the neurons in the Giant Fiber System of *Drosophila melanogaster* and their location relative to brain structures and relevant muscle groups. Arrows denote the regions where rectifying synapses are found. (B) A schematic of connections between the neurons that compose the GFS. GCI (orange) denotes Giant Commisural Interneurons. GF (red) denotes Giant Fiber. PSI (green) denotes Peripherally Synapsing Interneuron. TTM (brown) denotes Tergotrochanteral muscle, or leg muscle. TTMn (blue) denotes Tergotrochanteral Motor Neuron. DLMs (pink) denotes Dorsal Longitudinal Muscles, or wing muscles. DLMns (yellow) denotes Dorsal Longitudinal Motor Neurons. Rectifying synapses are found at the junctions between the GF and the PSI, and the GF and the TTMn, and are accompanied by chemical synapses. Non-Rectifying electric synapses are found between the GFs and the GCIs, the TTMn and the PSI, and the PSI and the DLMns. (Allen *et al.*, 2006). Reprinted from Sem. Cell Dev. Biol. 17. Allen, M.J., Godenschwege, T.A., Tanoyue, M.A., Phelan, P. Making an escape: Development and function of the *Drosophila* Giant Fiber System. Pages No. 31-41. © (2006), with permission from Elsevier.

## Methods

### *Primer Design and Mutagenesis*

*Drosophila* shaking-B (Lethal) was cloned into pSPJC2L and was a generous gift from Dr. Pauline Phelan (Univ. of Kent). Plasmid DNA was amplified after transformation into Top10 cells (Life Technologies Inc, Grand Island, NY) and overnight growth at 37 degrees in media supplemented with ampicillin. The following day, plasmid DNA was isolated using a Qiaprep kit (Qiagen Inc., Valencia, CA). Mutagenesis was performed using a Quikchange Lightning® mutagenesis kit (*Agilent Technologies - Stratagene Products, Santa Clara, CA*). Mutagenic primers were designed using the QuikChange® Primer Design Program (*Agilent Technologies - Stratagene Products, Santa Clara, CA*). Insertion primers were designed based on sequence analysis performed using ClustalW (Biology Workbench, SDSC). The rationale for primer design was as follows. First, a whole domain deletion of the N-Terminus of ShakB L (L2 through T19) was performed. Second, the whole N-terminus of ShakB N+16 (E2 through I24) was inserted into the construct lacking the ShakB L N-terminus, creating a hybrid ShakB L with the N-terminus of ShakB N+16. Mutagenesis reactions were performed as described in the Stratagene Quikchange Lightning protocol (*Agilent Technologies - Stratagene Products, Santa Clara, CA*). Mutations were confirmed by sequencing through the coding region (Roswell Park Cancer Institute DNA Sequencing Facility, *Buffalo, NY*) and Biology Workbench was used to align sequences and confirm that the desired insertions and deletions were created. Once DNA sequences were confirmed, constructs were used as templates to make RNA. Figure 7a shows the map of the vector pSPJC2L with ShakB L inserted within the multiple cloning region. Note the SP6 priming site for RNA polymerase is slightly upstream of the gene and can be used to transcribe RNA *in vitro*. The SP6 site was also used as the priming site for sequence analysis.

Figure 7b shows the P-element construct containing ShakB N+16, which is ideal for future studies involving *in vivo* analysis of Shaking B function. The amino acid sequences of ShakB L and ShakB N + 16 are compared in Figure 7c. The similar proteins are produced as transcript variants of the ShakB locus (Phelan and Starich, 2001).

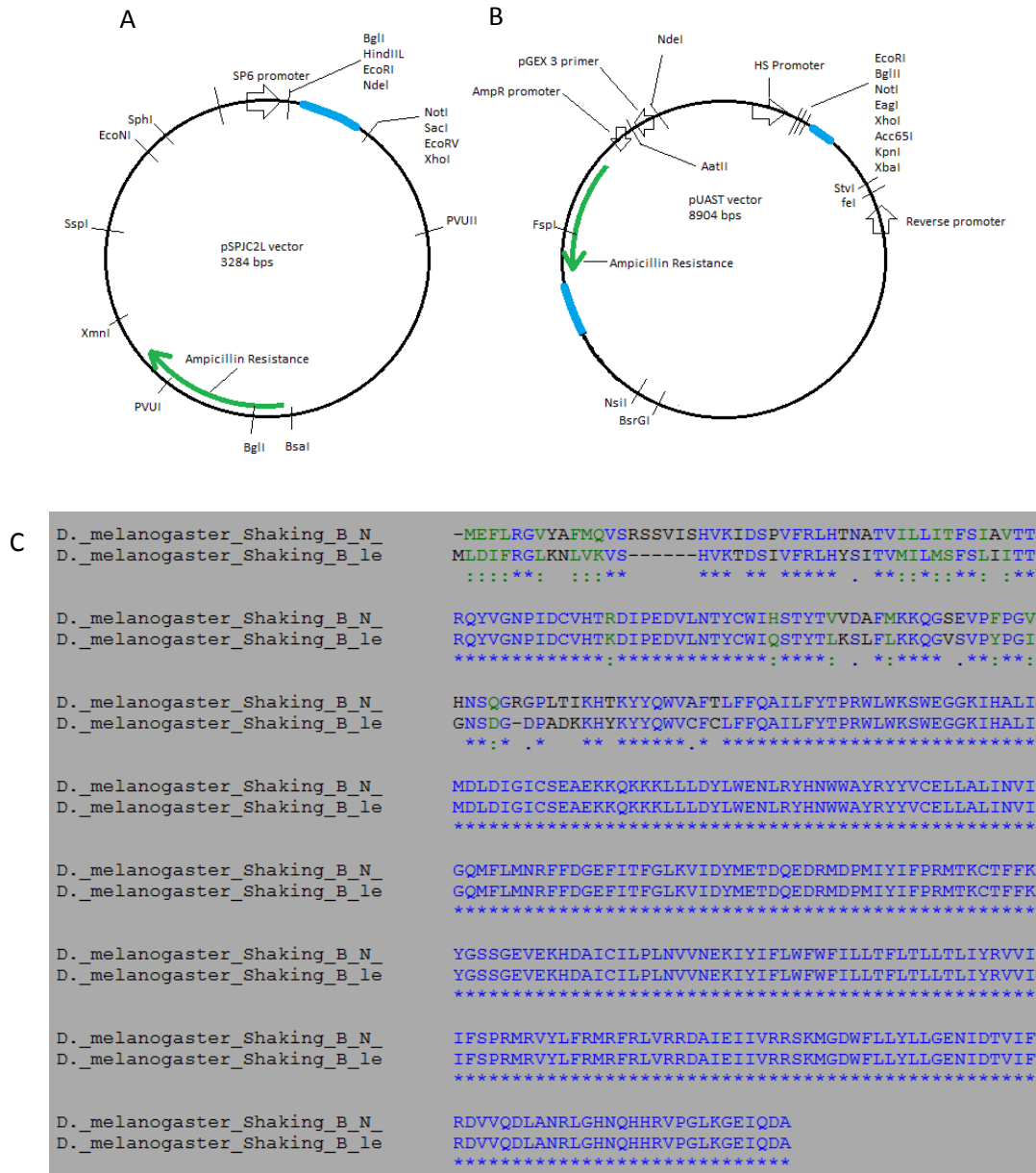


Figure 7

Figure 7. Vector maps of (A) Shaking B lethal and (B) Shaking B (N+16) showing the orientation of the genes in the vectors provided by Dr. Pauline Phelan (Univ. of Kent). Shaking B lethal is inserted in pSPJC2L and is downstream of the SP6 promoter used to synthesize RNA. The SP6 promoter is also the priming site used for sequencing. Shaking B (N+16) is inserted in pUAST, a vector that does not contain a priming site for RNA polymerase. This is a P-element vector suitable for the proposed in vivo studies in *Drosophila melanogaster*. (C) The sequences of Shaking B lethal (top) and Shaking B (N+16) differ in the first half of the protein but are identical from the end of M2 through to the carboxyl terminus.

In order to create the desired construct, a deletion of the entire N-terminus of ShakB L (residues L2-T19) was created using forward and reverse primers that complemented about 20 nucleotides on either side of the targeted deletion. The primers create a loop of DNA (the targeted deletion) that is not included in the extension process during PCR. Following the successful deletion, a region coding the amino terminus of ShakB N+16 was inserted. Forward and reverse insertion primers were designed, and each contained regions flanking the targeted insertion that were complementary to the ShakB L construct. In addition, the primers included a 69 nucleotide loop containing the sequence to be inserted. During PCR, the large insertion primer is extended creating a product that is 69 nucleotides longer than the template sequence. Insertion mutagenesis of a single residue in the same fashion of the larger insertion was used to correct an error in the initial insertion reaction. Figure 8 below shows a series of images illustrating the sequences of the chimeric constructs and their parent proteins.

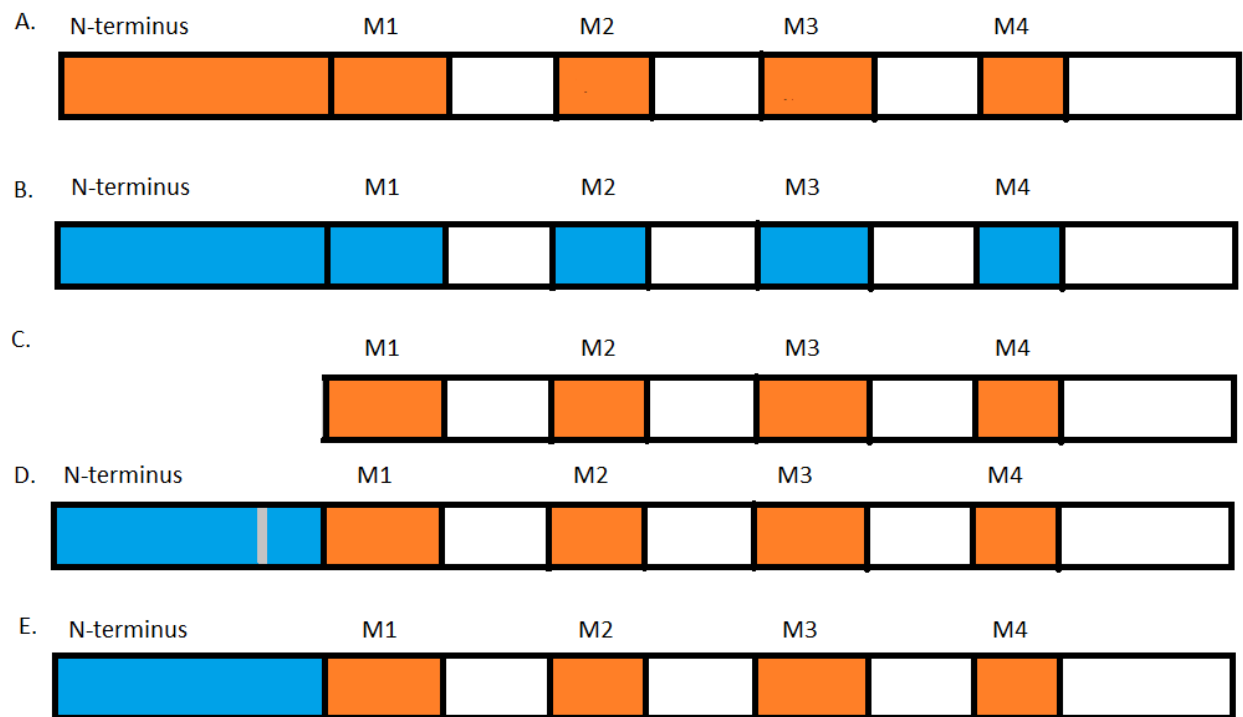


Figure 8

Figure 8. Illustrations of the various constructs used in this study. (A) ShakB L, noted in orange. (B) ShakB N+16, noted in blue. (C) Mutant construct “SBL-NTdel”, in which the N-terminus of ShakB L is deleted. The remainder of the protein is noted in orange, as it is a variation of ShakB L. (D) Mutant construct “SBL+N16NT-I19”, in which the N-terminus of Shakb N+16 (blue region) was inserted in the place of that of ShakB L, but without Isoleucine 19 (grey stripe). (E) Mutant construct “SBL+N16NT”, in which the missing Isoleucine is restored, resulting in a chimeric protein which had the “body” of ShakB L (orange) and the N-terminus of ShakB N+16 (blue).

### RNA Preparation

Prior to *in vitro* transcription, plasmid DNA was linearized with either XhoI or SacI. Linearization was verified by gel electrophoresis and a Geneclean kit (Q-Biogene Inc, Lachine, Quebec) was used to concentrate the DNA template. An agarose gel was run after each step to confirm successful linearization and concentration prior to assembling the *in vitro* transcription reaction and finally to confirm and quantify the transcribed RNA. All samples were run



alongside a Zip Ruler 1 DNA ladder (Fermentas Inc., Glen Burnie, MD) as a control for construct size and sample concentration. One microliter of DNA was run per lane. RNA was prepared using a standard mMessage mMachine RNA kit (Applied Biosystems/Ambion, Austin, TX). Sense RNA was synthesized using an SP6 promoter located upstream of the 5' end of the gene. RNA was purified with lithium chloride and quantified using gel electrophoresis and ethidium bromide staining through comparison to an RNA 250 control (Applied Biosystems/Ambion, Austin, TX).

#### *Oocyte Expression System.*

The oocyte expression system was used to assay properties of the ShakingB mutants. The technique of recording intercellular currents from paired *Xenopus* oocytes was carried out as described by Skerrett *et al.* (2001). Oocyte clusters were surgically extracted from *Xenopus laevis* according to an IACUC approved protocol. Oocytes were cleaned and digested in Oocyte Ringers 2 (OR2; 82.5 mM NaCl, 2 mM KCl, 1 mM MgCl<sub>2</sub>, 5 mM HEPES, pH 7.4). The oocyte clusters were treated with collagenase (*Type 1A, Sigma-Aldrich Corp. St. Louis MO*) to break down the connective tissue and allow for sorting. Only stage five or six oocytes were used for experimentation. Once the oocytes were sorted and separated, the follicle layer surrounding the cells was manually stripped off with two pairs of fine-tipped forceps (Skerrett, *et al.*, 2001). Oocytes were maintained in modified Barth's (MB) solution (88 mM NaCl, 1 mM KCl, 0.41 mM CaCl<sub>2</sub>, 0.82 mM MgSO<sub>4</sub>, 1 mM MgCl<sub>2</sub>, 0.33 mM Ca(NO<sub>3</sub>)<sub>2</sub>, 20 mM HEPES, pH 7.4) for injection, pairing and recording.

After the removal of the follicle layer, oocytes were injected with 0.5 ng (9 nl volume) of morpholino antisense oligonucleotide directed against *Xenopus* Cx38 (*Gene Tools*

LLC, Philomath, OR). The oligonucleotide serves to halt the expression of naturally occurring *Xenopus* connexin 38. After the injection with morpholino, the oocytes were placed in an incubator for approximately 12 hours at 17°C. The following day, oocytes were injected with RNA encoding the proteins of interest. A group of negative-control oocytes was also maintained. RNA was diluted to 125 ng /  $\mu$ l and 40 nl injection volume was used for each oocyte, establishing an estimated 5 ng of RNA per oocyte. In later experiments, low conductance measurements were required for accurate analysis of voltage-dependence and the amount of RNA injected was reduced by a half (2.5 ng / oocyte) or a quarter (1.25 ng / oocyte). Wildtype ShalB L has previously been expressed in oocytes using the construct in Figure 7a, in the lab of Dr. Phelan (Phelan *et al.*, 1998; Phelan *et al.*, 2008) and in our lab (DePriest *et al.*, 2011). ShalB L expresses consistently and robustly inducing intercellular conductance in the 50  $\mu$ S – 100  $\mu$ S range after RNA injections of 5 ng per oocyte.

To allow gap junctions to form between oocytes, the vitelline layer was manually removed and the oocytes were paired in shallow wells composed of agar and OR2 media.

To assess junctional conductance, paired oocytes were clamped at -20 mV using two Geneclamp Amplifiers (*Molecular Devices, Sunnyvale, CA*). One cell was pulsed to +80 mV and -120 mV eliciting a 2 second transjunctional current ( $I_j$ ), recorded as a clamping current in the partnered oocyte. Data were acquired and analyzed using pClamp10 software (*Molecular Devices, Sunnyvale, CA*). For a more detailed analysis of gating properties, a set of longer voltage steps was applied in 10 mV increments to a maximum transjunctional voltage ( $V_j$ ) of  $\pm 100$  mV. In both cases, currents were recorded and later measured using Clampfit software (*Molecular Devices, Sunnyvale, CA*) to establish conductance values both at the beginning and end of each voltage pulse. Initial currents were measured within the first 100 ms of the voltage

pulse, while final currents were measured at the end of the 2 second voltage pulse. In cases where accurate measurements of instantaneous current were hampered by membrane capacitance currents, exponential curves were carefully fit to the data and extrapolated to the time point corresponding to the start of the voltage pulse.

For studies of sensitivity to transmembrane voltage ( $V_m$ ), paired oocytes were clamped at identical holding potentials ranging from -100 mV to +60 mV while a transjunctional voltage was elicited as described above. Pairings between wildtype-injected oocytes and oocytes injected only with antisense morpholino (oligo/ShakB(L)) served as a negative control. A set of experiments was considered only if pairings between wildtype and antisense-injected oocytes failed to induce measurable intercellular currents.

## Results

### *Creating a Chimeric Innexin*

After deletion mutagenesis was performed on ShakB L and sequence analysis confirmed the deletion was successful, the construct was termed “SBL-NTdel”. The translated sequence of SBL-NTdel is shown in Figure 9A, aligned with the original ShakB L amino acid sequence.

The subsequent insertion mutagenesis reaction was successful but an error in primer design provided a new construct that incorporated all residues of the N-terminus of ShakB N + 16 with the exception of Ile19. This construct was named “SBL+N16NT-I19” (Figure 9b). In the final mutagenesis reaction, a short insertion primer was used to insert a codon corresponding to Ile19 resulting in a construct where the entire ShakB L N-terminus was replaced by that of ShakB N+16. This construct was named “SBL+N16NT” (Figure 9c).

A.

```

D._melanogaster_Shaking_B_le      MLDIFRGLKNLVKVSHVKTDSIVFRLHYSITVMILMSFSLIITTRQYVGN
SBL-20D_Translated_-_Longest      -----MDSIVFRLHYSITVMILMSFSLIITTRQYVGN
                                   *****
D._melanogaster_Shaking_B_le      PIDCVHTKDIPEDVLNTYCWIQSTYTLKSLFLKKQGVSVPPGIGNSDGD
SBL-20D_Translated_-_Longest      PIDCVHTKDIPEDVLNTYCWIQSTYTLKSLFLKKQGVSVPPGIGNSDGD
                                   *****

```

B.

```

D._melanogaster_Shaking_B_N_      MEFLRGVYAFMQVSRSSVISHVKIDSPVFRHLHTNATVIL
SBL_w/_n16nt_20B_Translated_      MEFLRGVYAFMQVSRSS-VSHVKIDSIIVFRLHYSITVMI
                                   *****

```

C.

```

D._melanogaster_Shaking_B_N_      MEFLRGVYAFMQVSRSSVISHVKIDSPVFRHLHTNATVILLITFSIAVTTR
Rep-I-A_Translated_-_Longest      MEFLRGVYAFMQVSRSSVISHVKIDSIIVFRLHYSITVMILMSFSLIITTR
                                   *****

```

Figure 9

Figure 9. Alignment of amino acid sequences relevant to the creation of a chimeric Shaking B lethal. (A) Shaking B lethal and the mutant construct “SBL-NTdel”. The upper sequence represents the first 100 amino acids of SBL, and the lower sequence is the mutated version demonstrating deletion of the amino terminus. Residues L2 through T19 of SBL were removed by deletion mutagenesis. (B) Alignment comparing amino acid sequences of Shaking B neural+16 to the construct “SBL+N16NT-I19”. The naturally occurring SBN+16 is on the top, while the mutant is on the bottom. The initial mutagenesis reaction failed to insert I19 of the N+16 N-terminus. Other mismatches in the alignment represent naturally occurring differences in the protein sequence of Shaking B Lethal (bottom) and Shaking B N+16 (top). (C) Amino acid sequence alignment comparing wildtype Shaking B Neural+16 with the mutant construct “SBL+N16NT”, in which the N-terminus of Shaking B lethal is replaced with the N-terminus of Shaking B Neural + 16. The wildtype N+16 sequence is on top and the N+16 N-terminus is comprised of residues M1 through I24.

### RNA Preparation

Figure 10 shows linearized DNA run alongside a Zip Ruler 1 DNA ladder (Fermentas Inc., Glen Burnie, MD) as a control for both construct size and sample concentration. All samples were successfully linearized. Agarose gels also confirmed the success of *in vitro* transcription,

as seen in the gel sample in Figure 11, where an RNA product is run alongside an RNA sample of known concentration (RNA control 250, Applied Biosystems/Ambion, Austin, TX).

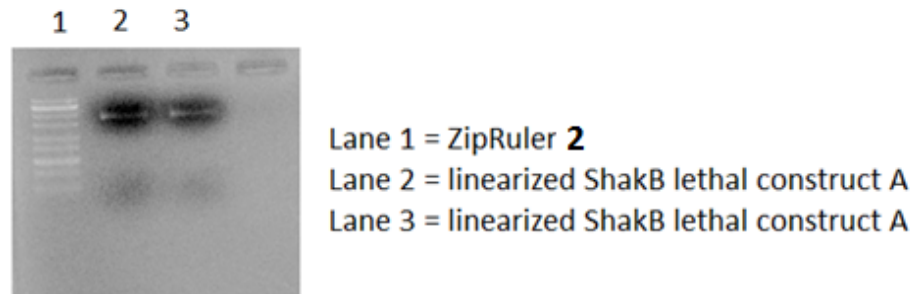


Figure 10

Figure 10. Agarose gel confirming the successful linearization of the plasmid DNA in lanes 2 and 3, which contain the mutant construct “SBL+N16NT”. Lane 1 contains the DNA ladder ZipRuler 2 (Fermentas Inc Glen Burnie, MD). The linearized DNA is about 4000 base pairs in length and is present at a concentration of about 50 ng per microliter.

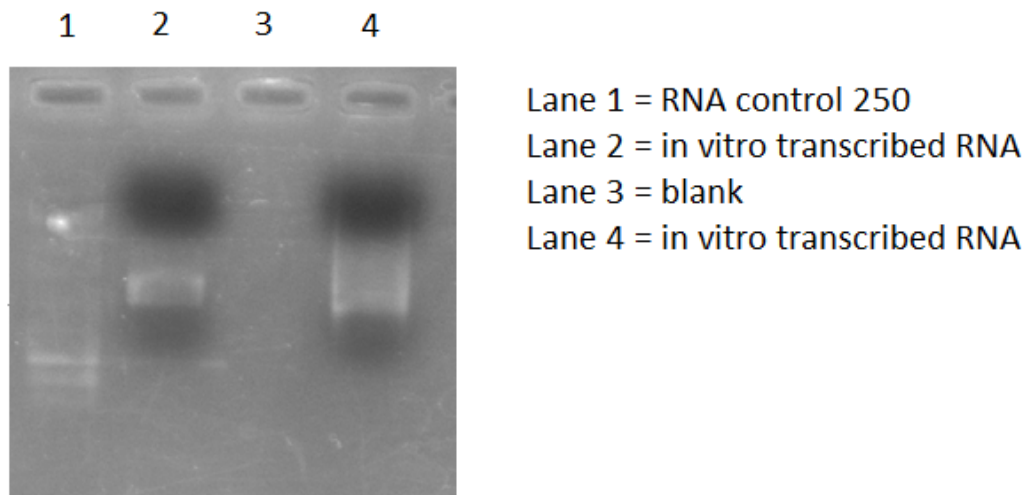


Figure 11

Figure 11. Agarose gel confirming the presence of RNA after in vitro transcription. Lane 1 shows the RNA 250 control while lanes 2 and 4 show RNA samples for Shaking B lethal. Since the gel is non-denaturing the RNA appears as a smeared band due to secondary structure. The estimated concentration based on comparison to the 250 ng /  $\mu$ l standard in Lane 1 is 300 ng /  $\mu$ l for the sample in Lane 2 and 400 ng /  $\mu$ l for the sample in Lane 4. RNA was later diluted to a concentration of about 125 ng /  $\mu$ l prior to injection.

## *Xenopus Oocyte Expression and Electrophysiology*

### *Deletion of the Amino Terminus*

In order to establish the necessity of an amino terminus for function, the SBL-NTdel was tested in oocytes. While ShakB L expressed robustly, inducing an average conductance above 100  $\mu$ S, the mutant failed to induce intercellular conductance when paired with itself. As shown in Figure 12a, the mutant-induced conductance is indistinguishable from non-injected controls, while wildtype ShakB L induced an average conductance of 140  $\mu$ S (n=3, SE = 32  $\mu$ S). The expression of wildtype ShakB L was typically high and exhibited a symmetrical response to voltage as expected (Figure 13a). Wildtype ShakB L paired with uninjected controls had a conductance of 0  $\mu$ S (n=4, SE = 0  $\mu$ S). Note that since all oocytes were first injected with a morpholino antisense oligonucleotide to reduce expression of endogenous connexins, the uninjected controls are referred to henceforth as “oligo controls”. Pairing of oocytes expressing the ShakB L, NT deletion (SBL-NTdel) were non-functional, having an average conductance of 0  $\mu$ S (n=3, SE = 0  $\mu$ S). A sample trace showing the “flat line” observed in the absence of intercellular coupling is shown in Figure 13b).

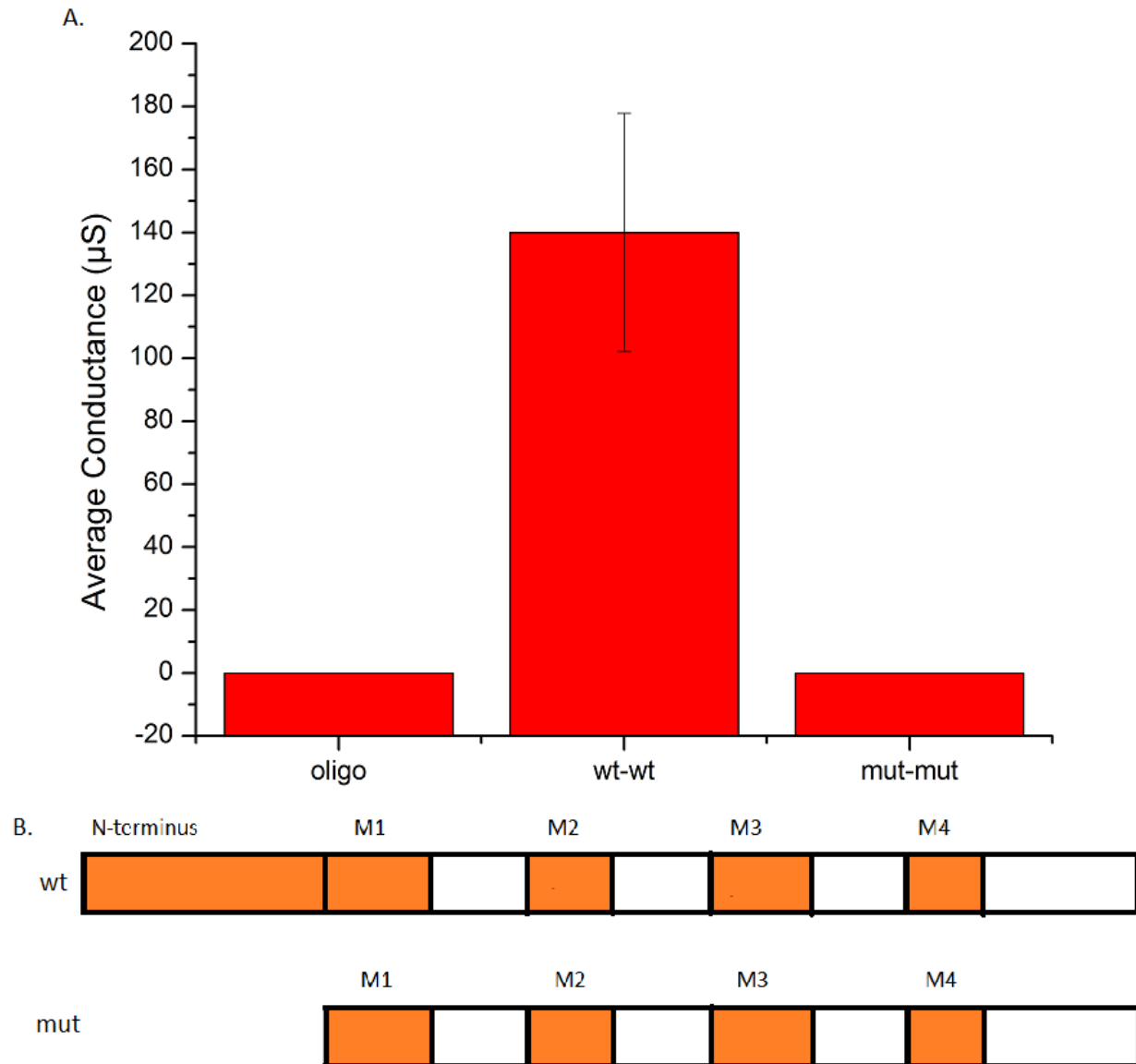
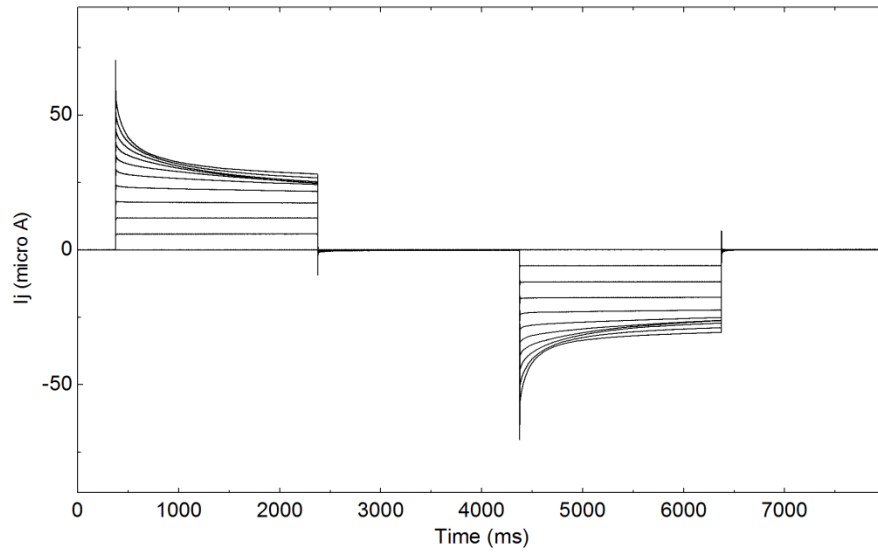


Figure 12

Figure 12. (A) Average conductances for the experimental series involving the mutant “SBL-NTdel” (deletion of the Shaking B (lethal) N-terminus). The oligo controls had an average conductance of 0  $\mu$ S ( $n=4$ ,  $SE=0$   $\mu$ S). The wildtype-wildtype pairings had an average conductance of 140  $\mu$ S ( $n=3$ ,  $SE=32.78$   $\mu$ S). Mutant-mutant pairings had an average conductance of 0  $\mu$ S ( $n=3$ ,  $SE=0$   $\mu$ S). (B) Graphic depicting the two constructs used in this experimental series; Wild type ShakB L (wt) and the mutant “SBL-NTdel” (mut).



A.



B.

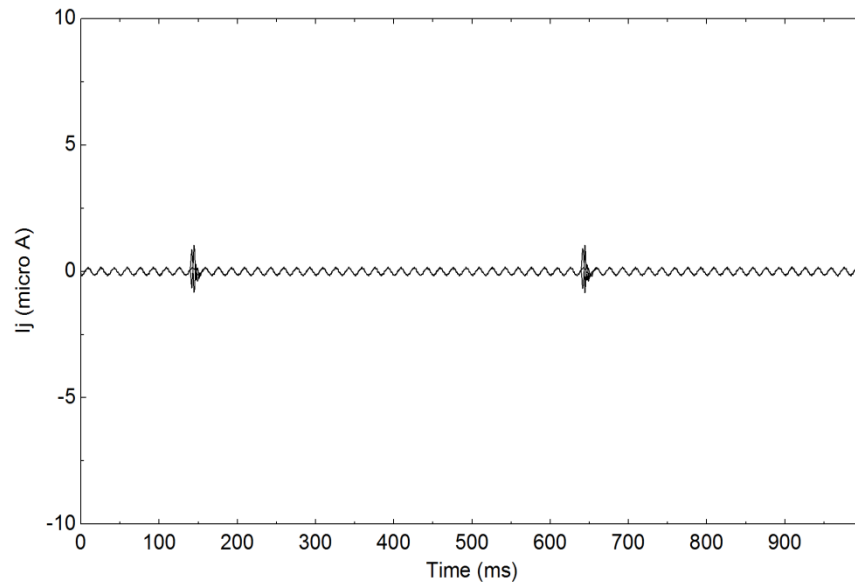
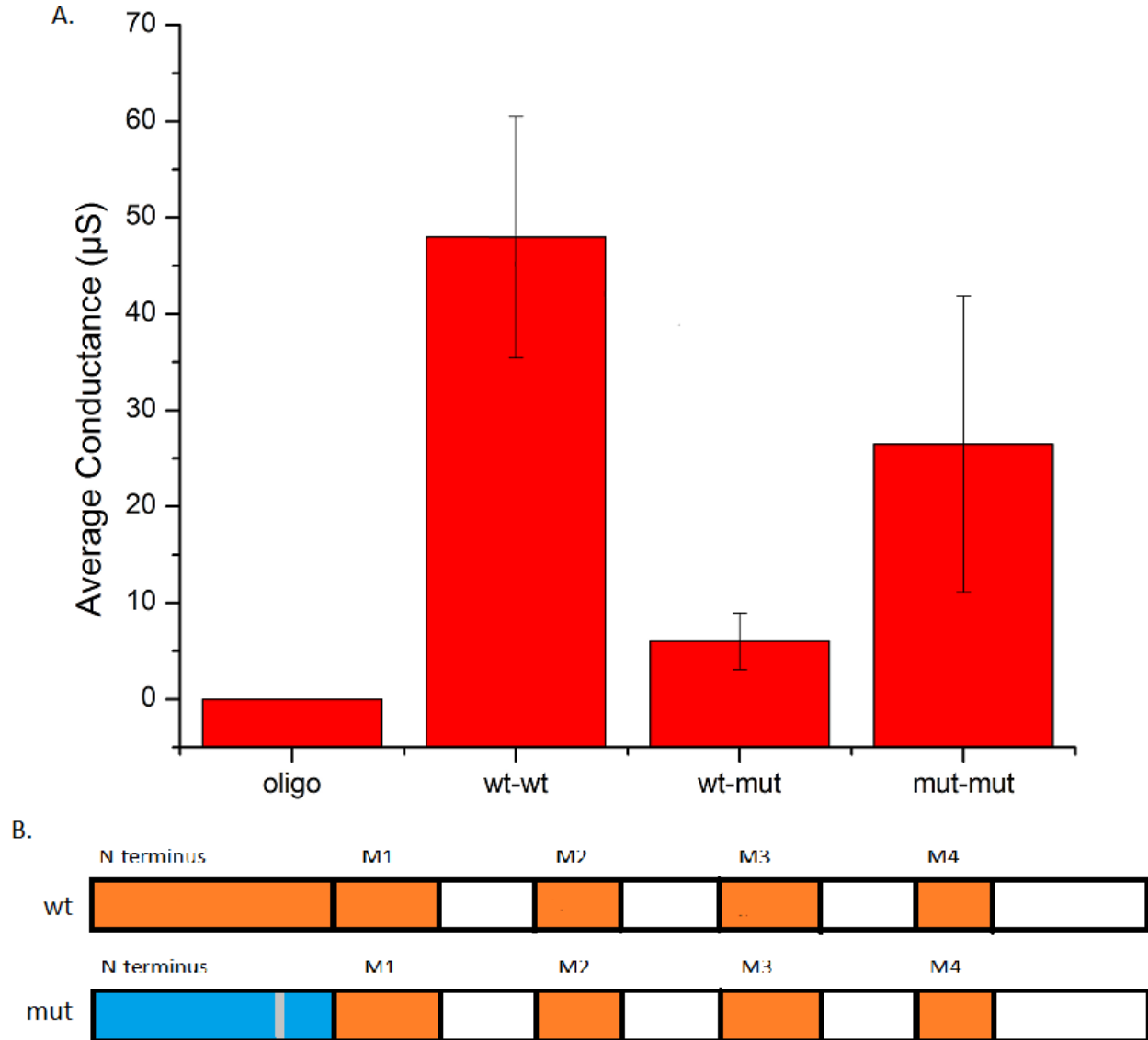


Figure 13

Figure 13. (A) A set of intercellular currents recorded from oocytes expressing wt Shaking B (lethal). Note the symmetrical response to voltage, which causes channels to close slowly over time. The currents display time- and voltage- dependent inactivation. (B) A set of currents recorded from oocytes expressing Shaking B lethal Nt-Del (N-terminal deletion). The mutant consistently failed to induce intercellular currents in oocytes.

*Insertion of ShakB N+16 Amino Terminus (missing I19)*

Electrophysiological testing of the construct “SBL+N16NT-I19” showed that the mutant was functional (Figure 14). In the experiment, oligo controls had an average conductance of 0  $\mu$ S (n=4, SE = 0  $\mu$ S), wildtype ShakB L pairings had an average conductance of 48  $\mu$ S (n=4, SE =12.5  $\mu$ S), pairings between wildtype ShakB L and SBL + N16NT-I19 had an average conductance of 6.02  $\mu$ S (n=5, SE= 2.95  $\mu$ S) while homotypic pairings of the mutant induced conductance of 26.5  $\mu$ S (n=4, SE=15.39  $\mu$ S).



**Figure 14**

Figure 14. (A) Average conductances in the experimental series using the mutant SBL+N16NT-I19 (replacement of the SBL N-terminus with a variant of the N-terminus of SBL N+16 which is missing I19). The oligo control had an average conductance of 0  $\mu$ S (n=4, SE = 0  $\mu$ S). The average conductance of the wildtype-wildtype pairings was 48  $\mu$ S (n=4, SE=12.5  $\mu$ S). The Wildtype-mutant pairing had an average conductance of 6.02  $\mu$ S (n=5, SE=2.95  $\mu$ S). The average conductance for the mutant-mutant pairings was 26.5  $\mu$ S (n=4, SE=15.39  $\mu$ S). (B) Graphic depicting the two constructs used in this experimental series; Wild type ShabB L (wt) and the mutant “SBL+N16NT-I19” (mut).

Interestingly, pairings between wildtype ShakB L and the mutant exhibited both asymmetrical gating and appeared to display instantaneous rectification. This is apparent in the current traces displayed in Figures 15 and 16. In heterotypic ShakB L/SBL + N16NT-I19 pairings, the channels gate strongly when the wildtype-expressing oocyte is relatively negative. Rather than inactivating in response to relative positive voltages, the channels activate slightly. In addition, the current level (and therefore junctional conductance) appears to be larger upon depolarization when measured at the start of the voltage pulse suggestive of “instantaneous rectification”.

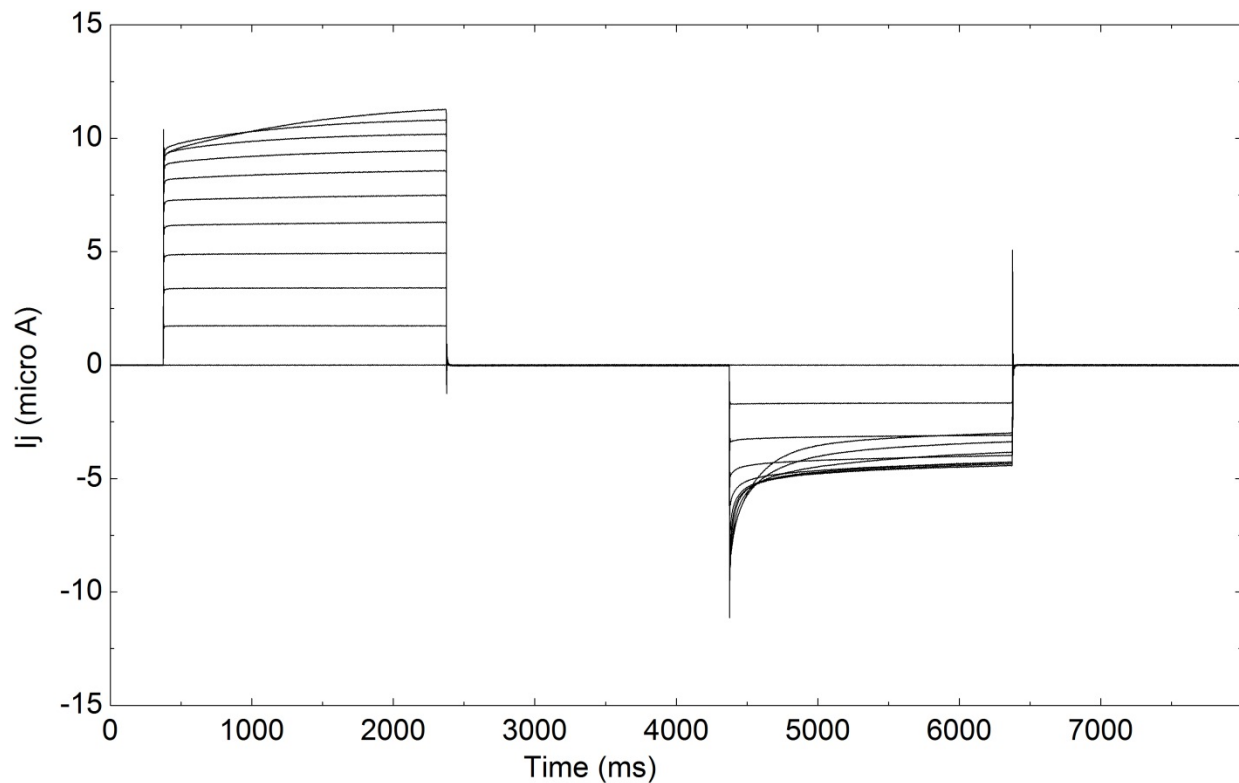


Figure 15

Figure 15. A set of current traces recorded from oocytes expressing heterotypic gap junction proteins Shaking B Lethal and Shaking BN16NT-I19. This recording was taken relative to the wildtype-expressing oocyte, meaning that outward currents represents the flow of positively charged ions or molecules out of the wildtype-expressing cell, or into the mutant-expressing oocyte. Note the asymmetric nature of the voltage-gating response, and also the apparent difference in instantaneous current flow at the start of the trace.

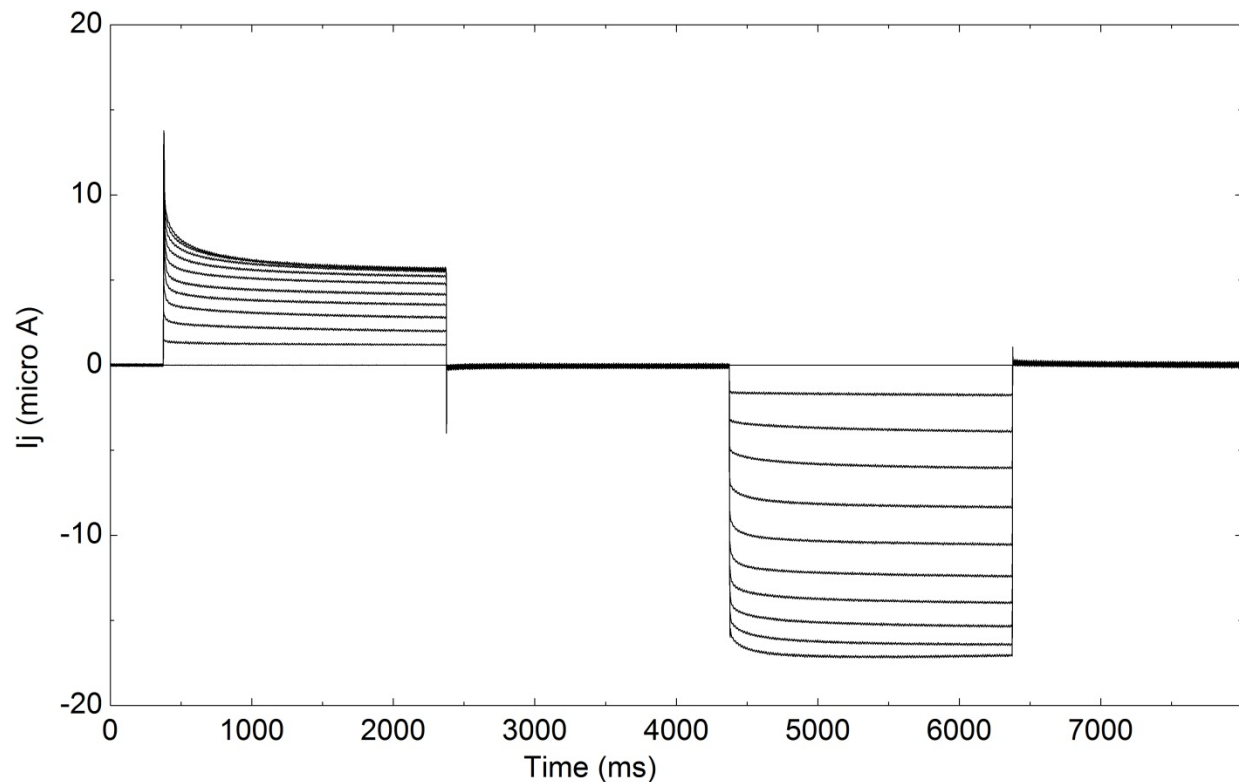


Figure 16

Figure 16. A set of current traces recorded from oocytes expressing heterotypic gap junction proteins Shaking B Lethal and Shaking BN16NT-I19. This recording was taken from the mutant- expressing oocyte, meaning that outward currents represent the flow of positively charged ions or molecules, out of the mutant-expressing cell or into the wildtype- expressing oocyte. Note the asymmetric nature of the voltage-gating response, and also the apparent difference in instantaneous current flow at the start of the trace.

To further investigate the properties of SBL + N16NT-I19, the oocyte holding potential was varied. In other experiments, oocytes were continuously clamped at -20 mV. In this experiment, currents were measured at four different holding potentials, -100 mV, -60 mV, -20 mV, and 20 mV. Variations in holding voltage did not strongly effect gating (see Figures 17 and 18) although it is not possible to rule out some minor influence of holding voltage. Physiologically such regulation could occur as the resting membrane potential of communicating cells was altered.

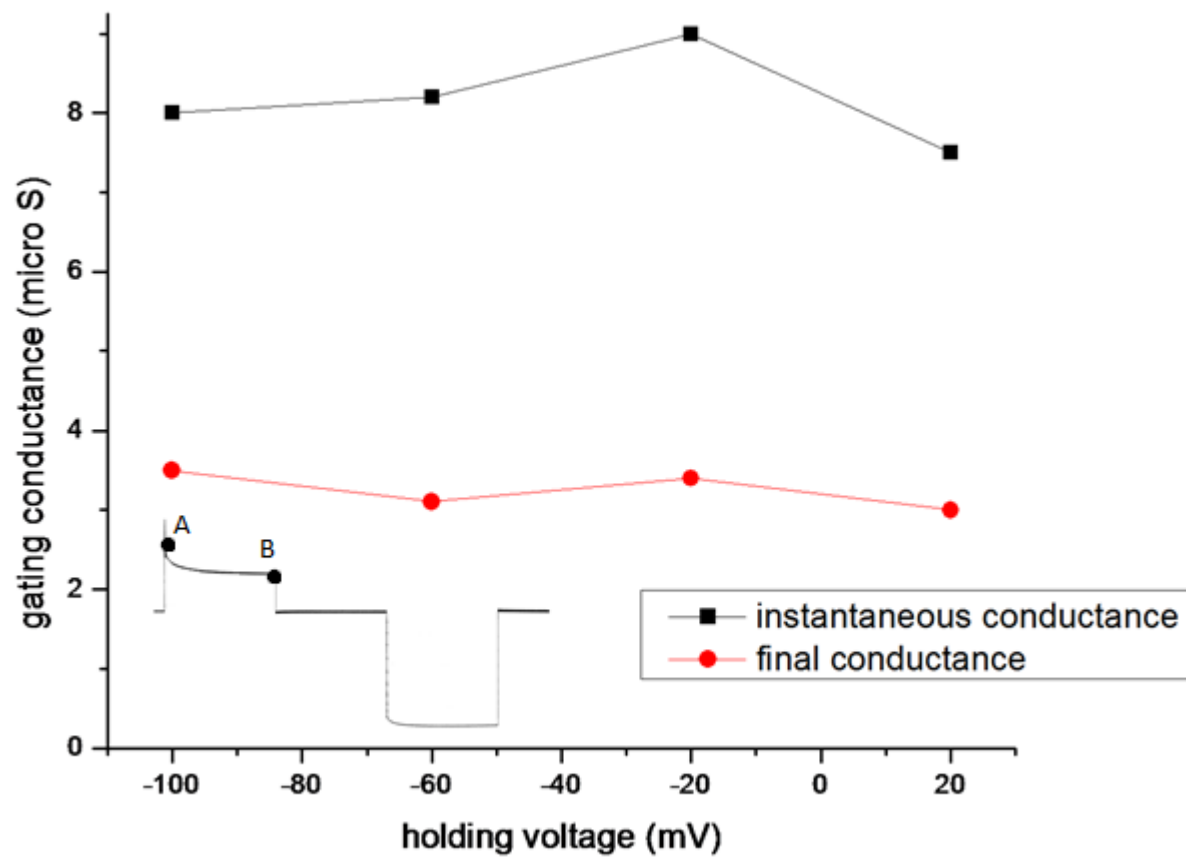


Figure 17

Figure 17. The effect of holding voltage ( $V_m$ ) on conductance. Instantaneous conductance and steady state (final) conductance are plotted as a function of holding voltage for oocytes expressing Shaking B lethal / SBL+N16NT-I19. Currents were measured relative to the wildtype- expressing oocyte and recordings were taken from the same pair of oocytes at holding voltages of -100 mV, -60 mV, -20 mV, and 20 mV. Instantaneous conductance was calculated from the current at the highest value, immediately after the capacitance spike (see A on the inset sample trace). Steady state (final) conductance was calculated from the current at at the highest value immediately before the end of the pulse (see B on the inset sample trace).

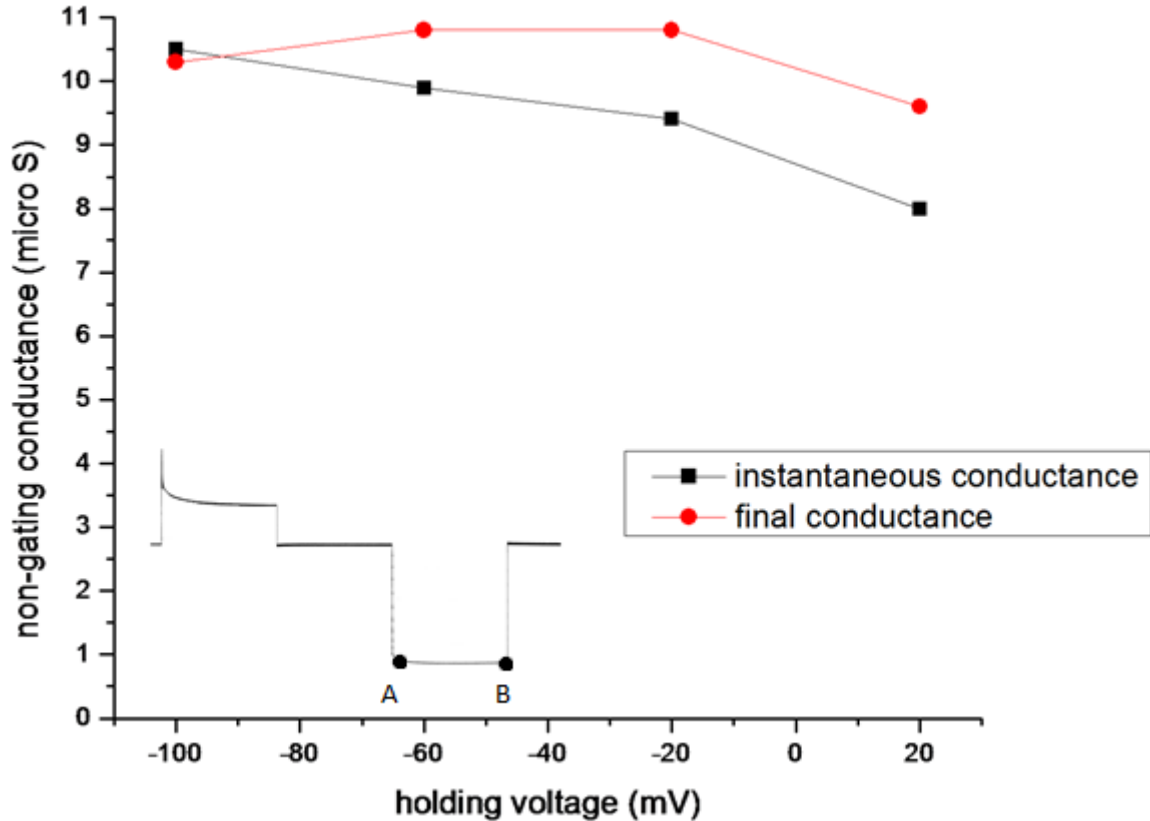


Figure 18

Figure 18. The effect of holding voltage ( $V_m$ ) on conductance. Instantaneous conductance and steady state (final) conductance are plotted as a function of holding voltage for oocytes expressing Shaking B lethal / SBL+N16NT-I19. Currents were measured relative to the mutant- expressing oocyte and recordings were taken from the same pair of oocytes at holding voltages of -100 mV, -60 mV, -20 mV, and 20 mV. Instantaneous conductance was calculated from the current at the highest value, immediately after the capacitance spike (see A on the inset sample trace). Steady state (final) conductance was calculated from the current at the highest value immediately before the end of the pulse (see B on the inset sample trace).

Figure 19 below summarizes the important changes induced in the chimeric innexin SBL N+16NT-I19 and compares these results to previous studies of Shaking B proteins. A side by side comparison of the traces obtained in this study and the traces obtained by Phelan *et al* (2008) confirm that the rectification observed in this study is similar to that observed in previous

studies when ShakB L is paired with ShakB N+16. Consistent with the observation of wildtype proteins in the studies by Phelan *et al* (2008), homotypic mutant/mutant pairings shows symmetric gating. Interestingly the SBL N+16NT-I19 shows similar gating to ShakB L in homotypic pairing, but when paired heterotypically with wild type ShakB L acts like ShakB N+16.



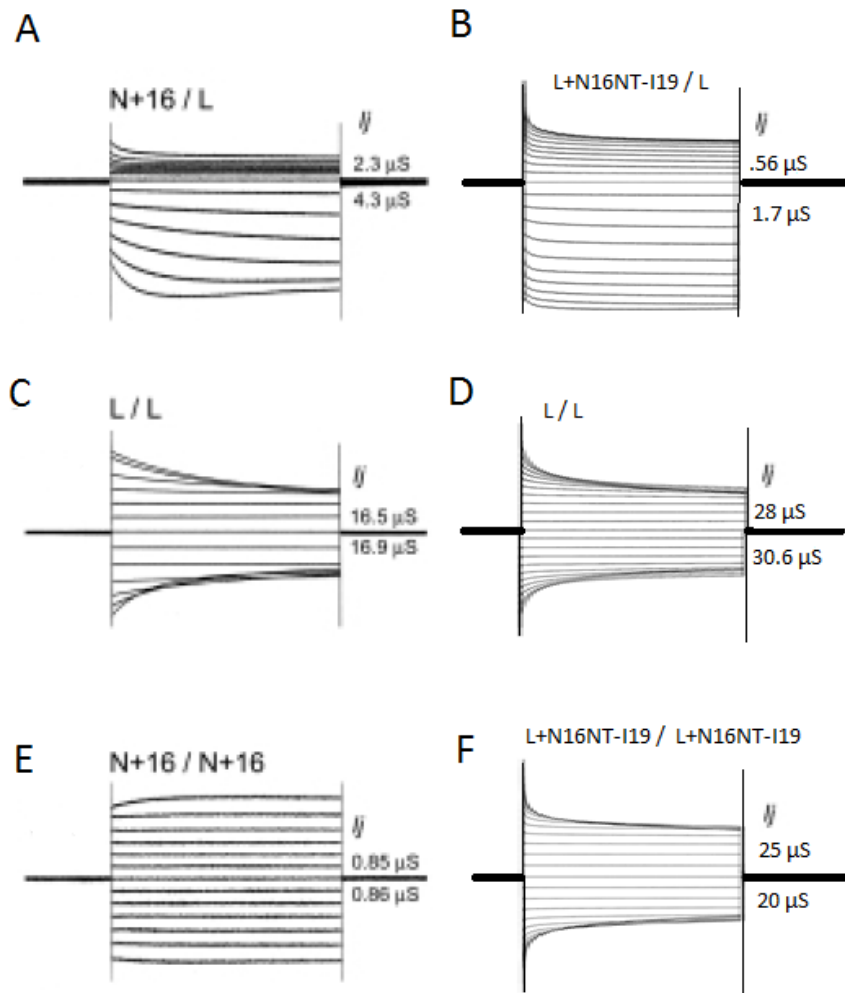


Figure 19

Figure 19. Comparisons of the junctional currents obtained by Phelan *et al* (2008; A,C,E) and in this study (B,D,F) for the mutant SBL+N16NT-I19. Data is recorded relative to the first construct listed above the trace (Construct 1 / Construct 2). Steady-state conductance values are noted to the right of each trace. Trace A is the naturally occurring rectifying junction composed of Shaker B N+16 and Shaker B lethal tested by Phelan *et al* (2008). Trace B represents currents of heterotypic pairings between SBL+N16NT-I19/ Shaker B lethal in this study. This junction rectifies in the same manner as the naturally occurring rectifier. Trace C represents homotypic Shaker B lethal/Shaker B lethal junctions tested by Phelan *et al* (2008). These respond symmetrically to applied voltage. Trace D represents homotypic currents of Shaker B lethal/Shaker B lethal in this study and these show the same response to applied voltage as when studied by Phelan *et al* (2008). Trace E represents homotypic Shaker B N+16 junctions (Phelan *et al.*, (2008). Trace F represents homotypic pairings between SBL+N16NT-I19. Note that when SBL+N16NT-I19 is paired with itself it behaves like wildtype Shaker B lethal, but when paired with wildtype Shaker B lethal, the mutant construct behaves like Shaker B N+16. Figures by Phelan *et al.*, (2008) are reprinted from Curr. Biol. 18, Phelan, P., Goulding, L.A., Tam, J.L.Y., Allen, M.J., Dawber, R.J., Davies, J.A., and Bacon J.P., Molecular Mechanism of Rectification in the *Drosophila* Giant Fiber System. Pages No. 1955-1960. © (2007), With permission from Elsevier.

*Complete chimeric Shaking B lethal with the amino terminus of Shaking B N+16*

In order to confirm that the interesting properties of SBL N+16NT-I19 could be attributed to the addition of the amino terminus of ShakB N+16 rather than the missing Ile19, a final construct was created using site-directed mutagenesis, reinserting the missing I19. Measurements of junctional conductance confirmed that the new construct SBL+N16NT produced functional gap junction channels and this information is summarized in a bar graph in Figure 20. The oligo control had an average conductance of 0  $\mu$ S (n=6, SE = 0  $\mu$ S). Wildtype-wildtype pairing in this series had an average conductance of 80.3  $\mu$ S (n=6, SE=5.7  $\mu$ S). The wildtype-mutant pairing had an average conductance of 78.14  $\mu$ S (n=7, SE=12.4  $\mu$ S).

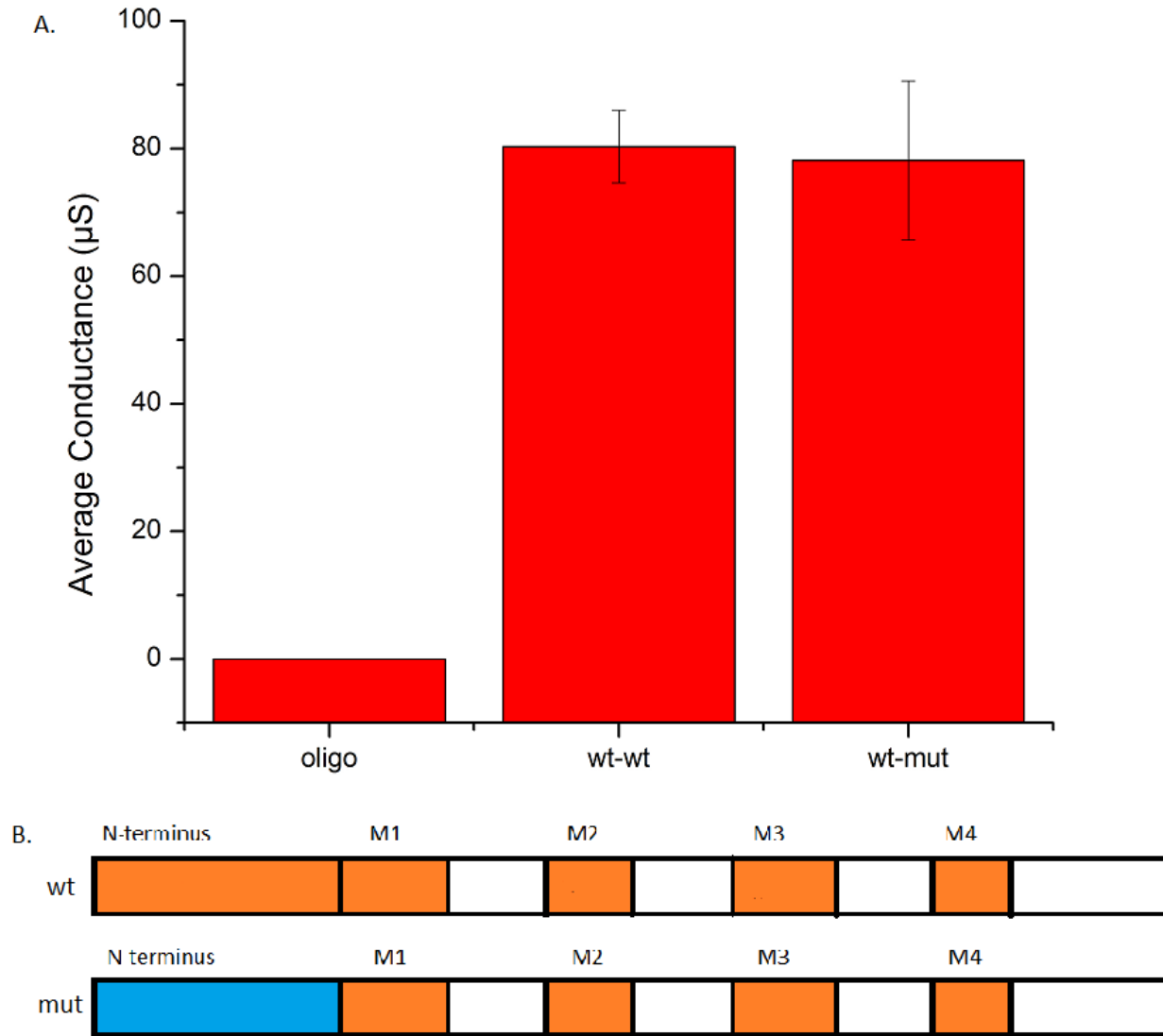


Figure 20

Figure 20. (A) Average conductances from the first experimental series involving the mutant construct “SBL+N16NT” (the replacement of the N-terminal of Shaking B lethal with the whole N-terminal of Shaking B N+16). The conductance of the oligo controls was 0  $\mu$ S ( $n=6$ , SE = 0  $\mu$ S). Wildtype-wildtype pairs had an average conductance of 80.3  $\mu$ S ( $n=6$ , SE=5.7  $\mu$ S). Wildtype-mutant pairs had an average conductance of 78.14  $\mu$ S ( $n=7$ , SE=12.4  $\mu$ S). (B) Graphic depicting the two constructs used in this experimental series; Wild type ShakB L (wt) and the mutant “SBL+N16NT” (mut).

To better assess voltage sensitivity of the chimera SBL+N16NT, another round of experiments was performed with reduced amounts of mutant RNA injected into the oocytes. As junctional conductance increases the relative contribution of series and access resistance

increases, resulting in reduced voltage drop across the junction (Wilders and Jongsma, 1992).

As demonstrated in the bar graph in Figure 21, reducing the RNA by a half or a quarter reduced coupling levels substantially. The oligo controls had an average conductance of 0  $\mu$ S (n=4, SE = 0  $\mu$ S). The homotypic wildtype ShalB L pairs injected with the standard 5 ng of RNA per oocyte had an average conductance of 82.2  $\mu$ S (n=5, SE=16  $\mu$ S). The pairs in which these wildtype-injected oocytes were paired with oocytes injected with half the amount of mutant RNA (1/2 conc, about 2.5 ng/oocyte) had an average conductance of 61  $\mu$ S (n=8, SE=14  $\mu$ S). The pairs in which the wildtype-injected oocytes were paired with oocytes injected with one quarter of the amount of RNA (1/4 conc., about 1.25 ng/oocyte) had an average conductance of 48  $\mu$ S (n=8, SE=16  $\mu$ S). Ideally, voltage-dependence should be studied at conductance below 10  $\mu$ S. Hence, oocyte pairs with conductance in the lower range will be selected for more detailed analyses of gating, specifically construction of a G<sub>j</sub> (*junctional conductance*) versus V<sub>j</sub> (*transjunctional voltage*) plot. Such plots are often fit with a Boltzman equation to determine parameters of V<sub>1/2</sub> and G<sub>min</sub>, standard indicators of the voltage at which half-maximal inactivation occurs and the minimal conductance induced by voltage, respectively.

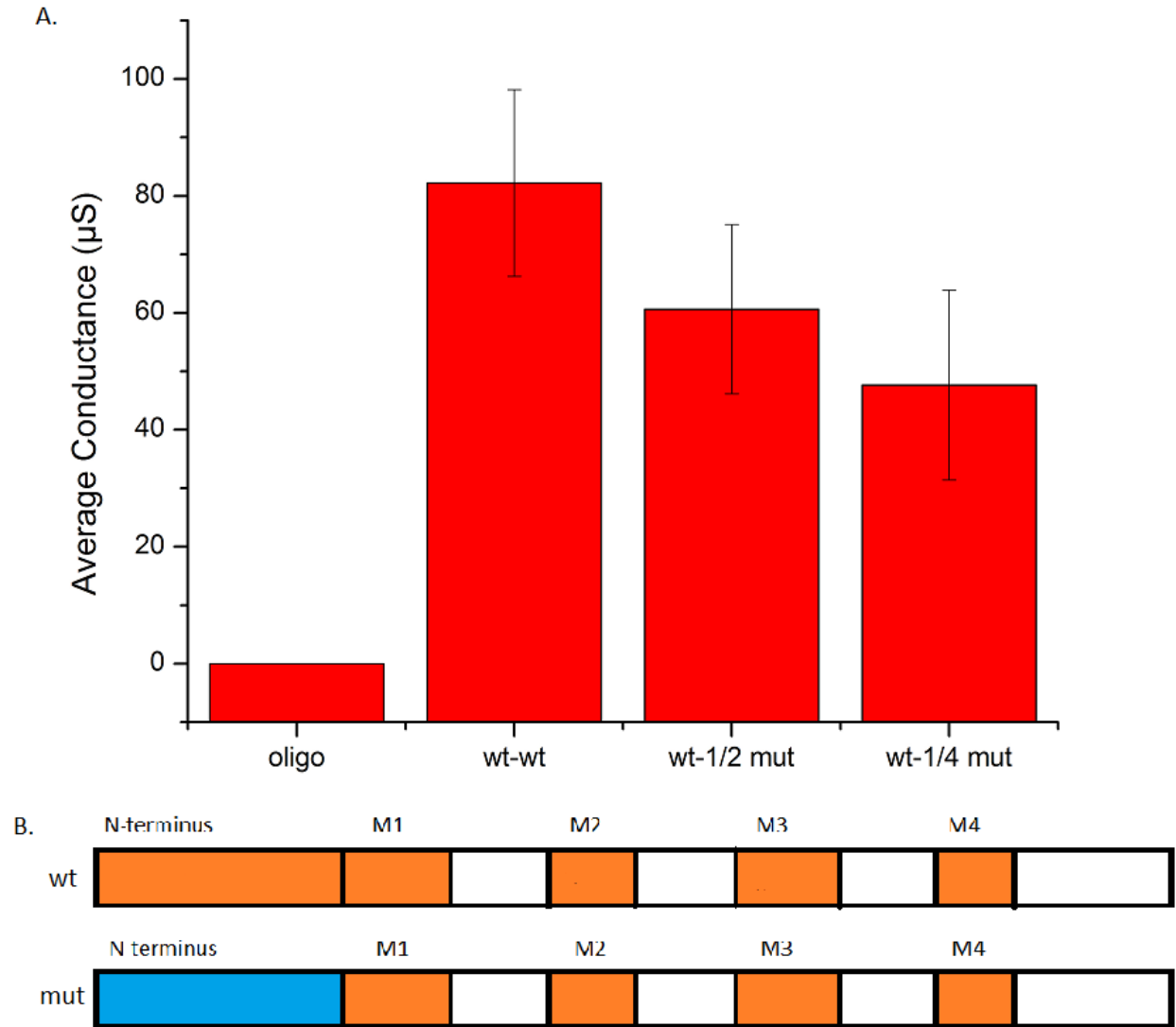


Figure 21

Figure 21. (A) Average conductances from the second experimental series involving the mutant construct SBL+N16NT. RNA encoding wildtype Shaking B lethal was injected at the standard amount (1.25 ng / oocyte), while the amount of RNA for the mutant was reduced by a half (half conc, about 0.6 ng/oocyte) and a quarter (1/4 conc, about 0.3 ng/oocyte). The average conductance of oligo control was 0  $\mu$ S (n=4, SE = 0  $\mu$ S). Homotypic wildtype/wild type pairs had an average conductance of 82  $\mu$ S (n=5, SE=16  $\mu$ S). The average for wildtype/mutant (half conc.) was 61  $\mu$ S (n=8, SE=14  $\mu$ S) while the average conductance for wildtype/mutant (1/4 conc.) was 48  $\mu$ S (n=8, SE=16  $\mu$ S). (B) Graphic depicting the two constructs used in this experimental series; Wild type ShkB L (wt) and the mutant “SBL+N16NT” (mut).

Current traces recorded from the chimera SBL+N16NT are shown in Figures 22, 23 and 24. Regardless of the RNA concentration, the mutant induced currents that gated asymmetrically when paired with wildtype ShakB L (Figures 22 and 23) but gated symmetrically, with characteristics similar to those of wildtype ShakB L, when paired homotypically (Figure 24). Side by side comparisons of the traces obtained in this study and the traces obtained by Phelan *et al* (2008) confirm that the chimera has gating properties similar to those of ShakB N+16 when paired heterotypically. In homotypic pairings, the mutant behaves similarly to wildtype ShakB L. It is also of note that the behavior of SBL+N16NT-I19 appears very similar to SBL+N16NT, and deletion of the isoleucine did not alter the function of the channel.

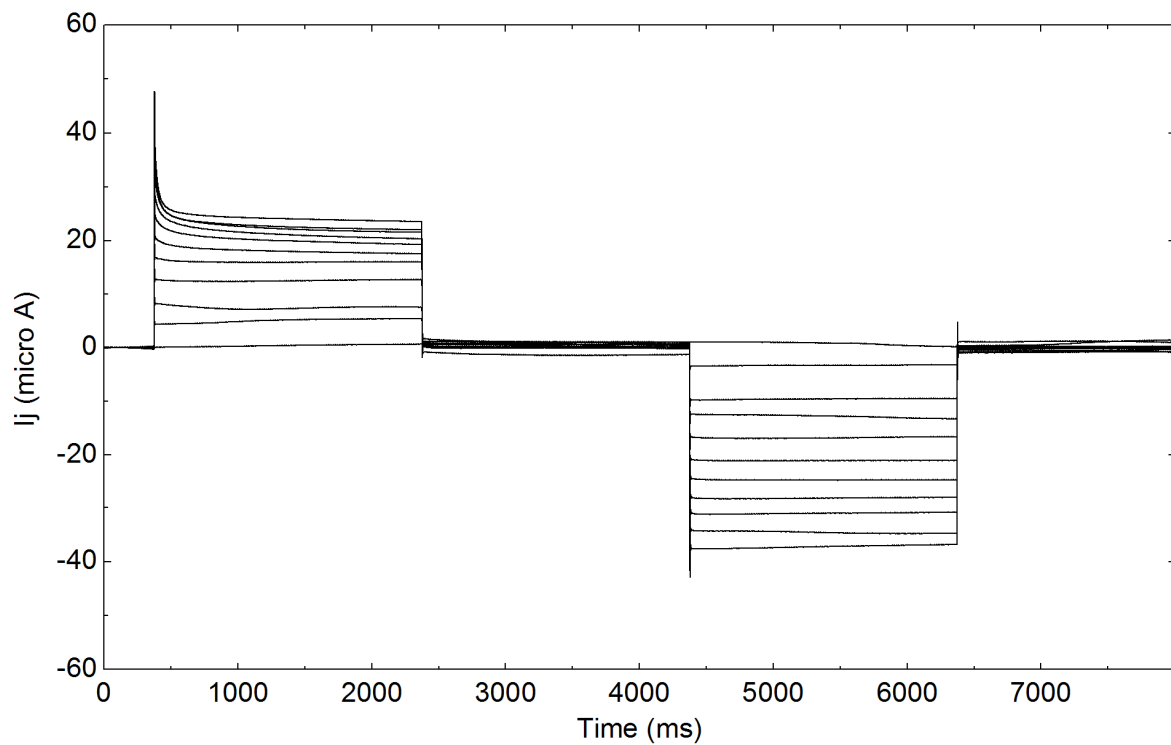


Figure 22

Figure 22. Example set of current traces recorded from heterotypic Shaking B lethal/SBL+N16NT pairs. Currents are shown relative to the mutant-expressing oocyte. The traces show the asymmetrical nature of the voltage response, and apparent instantaneous rectification.

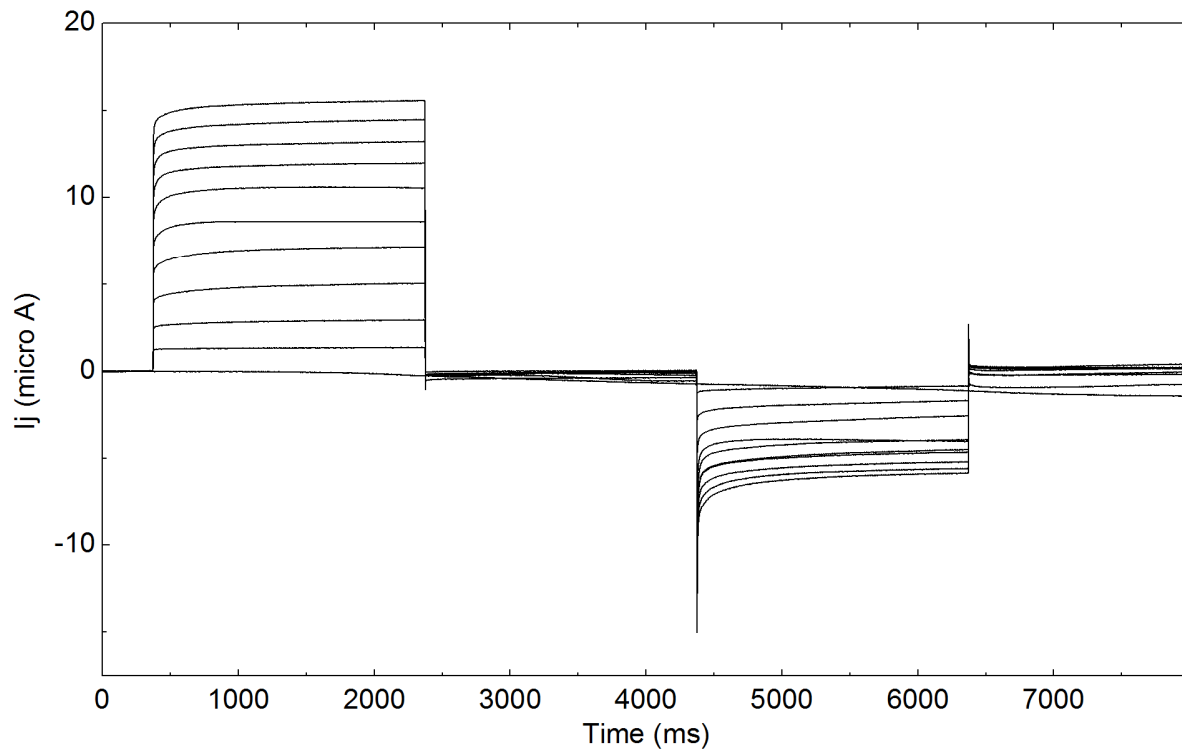


Figure 23

Figure 23. Example set of current traces recorded from heterotypic Shaking B lethal/SBL+N16NT pairs. Currents are shown relative to the wildtype-expressing oocyte. The traces show the asymmetrical nature of the voltage response, and appear to demonstrate instantaneous rectification

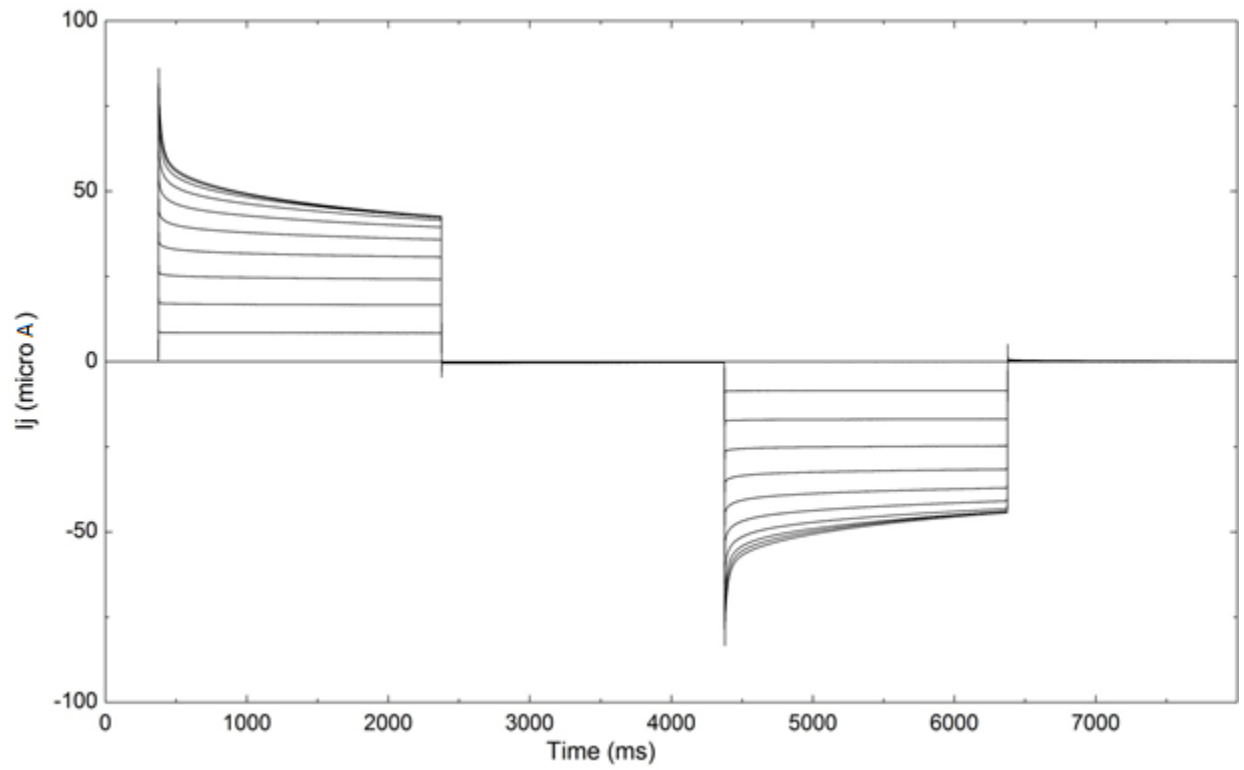


Figure 24

Figure 24. Example set of current traces recorded from homotypic SBL+N16NT/SBL+N16NT pairs. Currents are symmetric and resemble those of wildtype ShakingB lethal.



## Discussion

The chimera SBL+N16NT is a protein composed of ShakB L, with the N-terminus of ShakB N+16. The chimera was used to investigate the role of the N- terminus in electrical rectification at heterotypic ShakB L/ShakB N+16 junctions. Phelan *et al* (2008) recently showed that in the Giant Fiber System of *Drosophila*, ShakB(N+16) is expressed presynaptically in GFI's, while ShakB(L) is expressed in postsynaptic TTMn's. The two variants of ShakB, assemble to produce rectifying heterotypic gap junctions, the properties of which were investigated after expression in *Xenopus* oocytes (Phelan *et al.*, 2008). The chimeric construct SBL+N16NT was expressed in *Xenopus* oocytes to study interactions with wildtype ShakB L. The chimera expressed robustly and readily formed heterotypic junctions with ShakB L. The properties of the heterotypic junctions closely mimic the rectifying synapses observed by Phelan *et al.* (2008). The data supports the hypothesis that the N-terminus imparts properties that underlie rectification at heterotypic junctions.

## Coupling Levels

The average conductance values in the experiments provide information about the expression and function of mutant constructs. Each experimental series was performed using a single batch of oocytes obtained from the same frog in the same surgery. Despite efforts to minimize variability in this way, a wide range of conductance values were observed within each group. This variability can be attributed to variable health of oocytes, pre- and post-injection, or inconsistency in injection of volume of RNA (Skerrett *et al.*, 2001). In all experiments presented, most oocytes appeared healthy after injection and pairing and since a quantitative

analysis of conductance levels was not necessary, the large standard errors do not influence interpretation of the results.

#### *Analysis of the Mutant SBL-NTdel*

The analysis of SBL-NTdel demonstrated for the first time that removal of the N-terminus of an innexin results in loss of function. The average conductance for the mutant-mutant pairs was 0  $\mu$ S and an example trace shown in Figure 13 demonstrates only background noise in the paired oocytes. Although it is clear that the mutant is non-functional it is not clear whether loss of function results from problems with translation, insertion, trafficking to the membrane, docking or gating.

The deletion of the N-terminus of ShakB (L) removed 20 amino acids from the primary protein structure. It is possible that some of these residues play a role in protein folding and their loss prevents the rest of the protein from assuming the proper structure and function. Localization failure could occur for multiple reasons. If the protein is misfolded, it may not traffic properly and/or may fail to be inserted into the membrane. It is also possible that the protein does manage to fold properly, however the N-terminus plays a role in trafficking. This is particularly likely in light of the 2008 study by Kyle *et al*, which demonstrated that removal of a significant portion of the N-terminus of connexin 37 caused failure to localize. The final possibility is that the N-terminal domain is crucial for gating in the Shaking B innexins, and that removal of the domain caused a loss of gating capability. This has been observed for connexins, where removal of a large portion of the N-terminus eliminates function, and at the same time decreases the mass found within the pore in comparison to unaltered proteins (Oshima *et al*, 2008). It has been proposed that in connexins, the N-terminus folds up into the pore acting as a

plug to close the channel (Maeda *et al.*, 2009) or that the N-terminus holds the pore open under certain circumstances (Oshima *et al.*, 2008).

The exact reason for this loss of function can be determined in future experiments. A GFP tag on the C-terminus of the mutant would allow visualization of the protein and determination of the degree of localization to the membrane. GFP-tagged membrane proteins have been studied in oocytes using confocal microscopy, which allows visualization despite the yolk reserves within the cell (Limon *et al.*, 2007). If the proteins do localize to the membrane properly but fail to form gap junctions, the presence or absence of plaques can be studied using electron or atomic force microscopy as demonstrated by Yu *et al* (2007). If the channels are found to traffic, localize and form plaques successfully then the deletion of the N-terminus is likely to result in loss of function due to effects on gating.

#### *Analysis of the Mutants SBL+N16NT-I19 and SBL+N16NT*

The mutant construct SBL+N16NT-I19 represented a first attempt to replace the N-terminus of ShabB Lethal with that of N+16. Unfortunately, the codon for isoleucine 19 was missing in the mutagenesis primer. Despite the mistake, the mutant was tested and was found to be functional. When it was paired with wildtype ShabB L, the junction acted as a rectifier suggesting that the N-terminus did carry properties essential for rectification.

As shown in Figure 19, several interesting observations are highlighted through a side by side comparison of the traces obtained by Phelan *et al* (2008) and the traces obtained for SBL+N16NT-I19 in this experiment. First, the rectifying traces show very similar patterns when compared to each other. The fact that the data obtained in this study matches very closely the gating pattern of previously characterized rectifying junction suggests that the N-terminal

domain plays a significant role in the properties underlying rectification. It is very interesting to note that homotypic pairings of the SBL+N16NT-I19 mutant induce gating similar to that of wildtype ShabB L. This is in stark contrast to the behavior in heterotypic pairings where the mutant behaves similar to ShabB N+16. It appears that a significant part of the mechanism that drives rectification is imparted by the N-terminus, but the N-terminus plays little role in voltage-dependent gating of homotypic junctions. This provides evidence that rectification is unrelated to the gating mechanisms underlying  $V_j$ -dependent channel inactivation.

Analyses of the functional elements and structural motifs of the N-terminus suggest that this missing isoleucine may be irrelevant. Firstly, one of the crucial areas of the N-terminus is believed to be the charged residue in site 2 of the n-terminal chain (Oh, *et al.* 2000; Maeda *et al.*, 2009). This is unchanged from the normal N-terminal sequence for ShabB N+16, and is therefore unlikely to alter the expected gating pattern that can be expected in the whole N-terminal replacement tests. Secondly, predictions of the structure of the protein according to the model by Holley and Karplus (1989) suggest that the missing Isoleucine would not directly interfere in function. The model predicts the presence of two helices, one large helix in the first segment of the N-terminus, and a smaller four residue helix near the N-terminal/M1 boundary, much like the structure of the connexin 37 N-terminus (Kyle *et al.*, 2009). The missing isoleucine would be found in the short alpha helix that is likely to be the region that acts as a hinge in the physical movement of the larger helix of the N-terminal in and out of the pore, allowing for interactions with the pore lining helices (Kyle *et al.*, 2009; Maeda *et al.*, 2009). The model predicts that the loss of Isoleucine 19 will not impact the integrity of the short helix, and since the area that would be expected to interact with the pore lining helices is intact, there should be no significant variation between the traces observed for this construct and the whole

N-terminal replacement. This suggests that the rectification observed in this construct is genuine.

The construct SBL+N16NT represents a chimera of ShabB L with the N-terminus of ShabB N+16. The channels expressed robustly and displayed rectification in heterotypic pairing with wildtype ShabB L. The rectification is again similar to that observed by Phelan *et al* (2008) and this is apparent in the side-by-side comparison in Figure 25. The results are also similar to those obtained for the construct SBL+N16NT-I19. A set of traces is compiled in Figure 26 where the mutant constructs SBL+N16NT-I19 and SBL+N16NT are compared to one another, and also to the recordings of Phelan *et al.* (2008). The constructs display a similar pattern of rectification in heterotypic junctions and display similar gating responses in homotypic junctions. The similarity confirms that the missing I19 in SBL+N16NT-I19 is not crucial for gating or rectification. The observations further support the hypothesis that the N-terminal domain plays a key role in rectification in innexin channels.

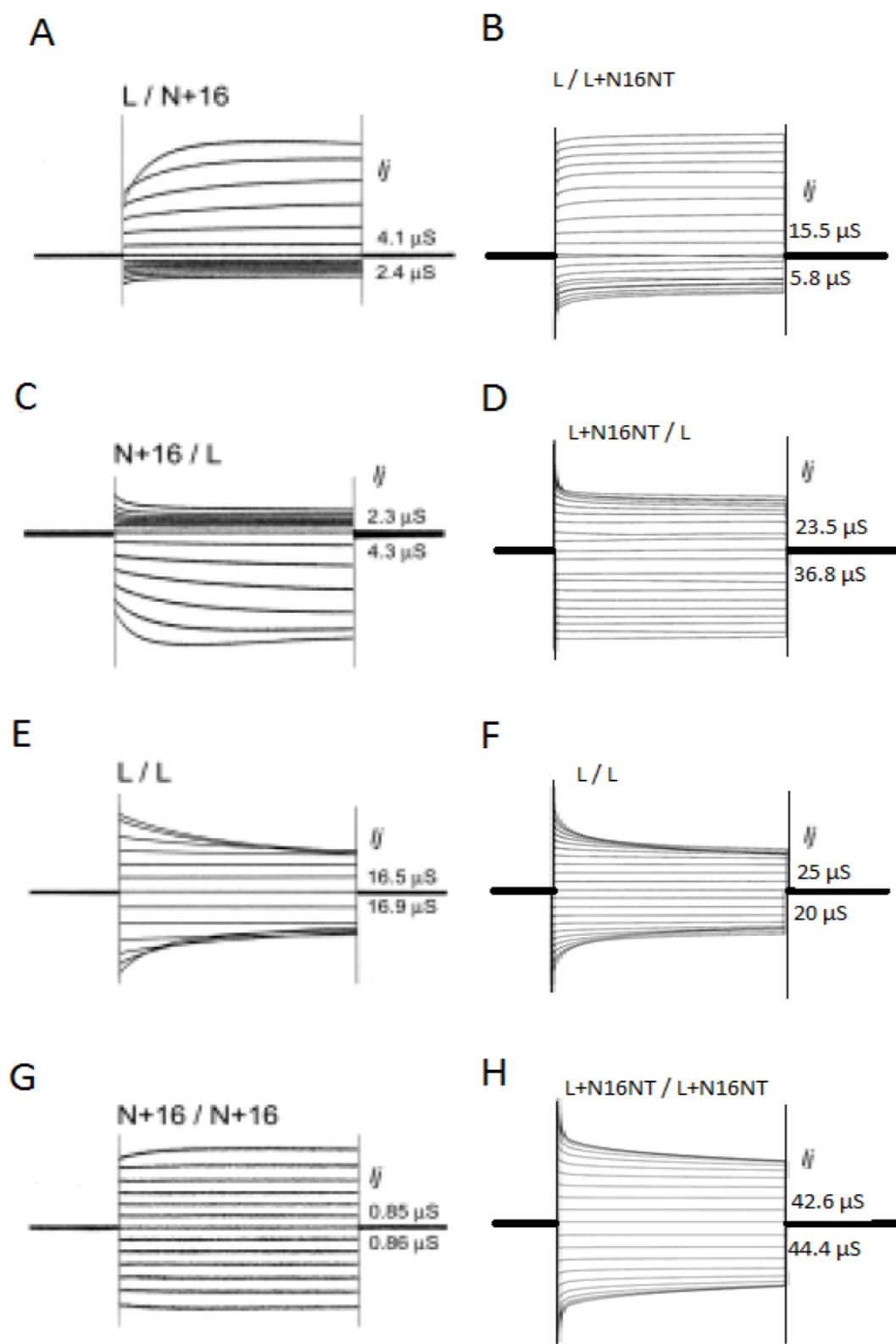


Figure 25

Figure 25. Side by side comparisons of the traces obtained by Phelan *et al* (2008; A,C,E,G) and in this study for SBL+N16NT (B,D,F,H). The first construct listed above the trace (Construct 1 / Construct 2) is represented on the bottom half of the trace, and the second half is represented on the top half of the trace. Steady state conductance values are noted to the right of each trace. Trace A represents the rectifying junction composed of Shaking B lethal and ShakB N+16 demonstrated by Phelan *et al* (2008). Trace B represents coupling of Shaking B lethal and SBL+N16NT in this study. This junction rectifies in the same manner as that observed by Phelan *et al.* (2008). Trace C is the rectifying junction composed of ShakB N+16 and ShakB L tested by Phelan *et al* (2008), and is the same junction type as shown in trace A, opposite polarity. Trace D represents coupling between SBL+N16NT and Shaking B lethal, and is the same junction as seen in trace B, opposite polarity. This junction rectifies in the same manner as the naturally occurring rectifier. Trace E represents homotypic Shaking B lethal/ Shaking B lethal junctions tested by Phelan *et al* (2008). The response to voltage is symmetric. Trace F represents the Shaking B lethal/ Shaking B lethal junctions tested in this study. The results match those obtained by Phelan *et al* (2008). Trace G represents homotypic junctions formed by ShakB N+16/ShakB N+16 (Phelan *et al.*,2008). Trace H represents currents recorded from the homotypic junctions composed of the chimeric protein SBL+N16NT/ SBL+N16NT. Note that when paired with itself, the mutant behaves like wildtype Shaking B lethal, but when paired with wildtype Shaking B lethal, the mutant behaves like ShakB N+16. Figures from Phelan *et al.*, (2008) are reprinted from Curr. Biol. 18, Phelan, P., Goulding, L.A., Tam, J.L.Y., Allen, M.J., Dawber, R.J., Davies, J.A., and Bacon J.P., Molecular Mechanism of Rectification in the *Drosophila* Giant Fiber System. Pages No. 1955-1960. © (2007), With permission from Elsevier.

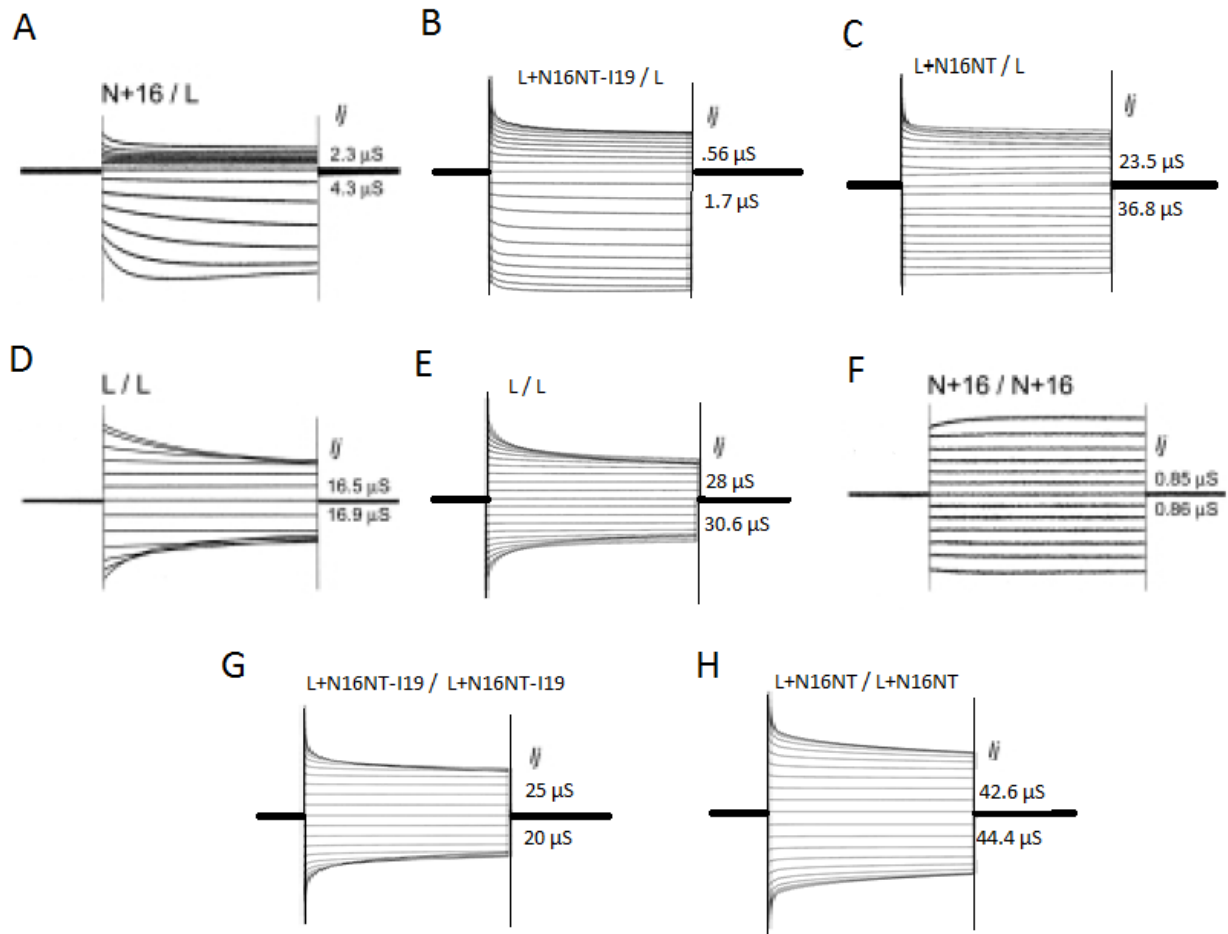


Figure 26

Figure 26. Side by side comparisons of the mutant traces obtained in this study (B,C,G,H) and the traces obtained by Phelan *et al.*, in 2008 (A,D,E,F). The first construct listed above the trace (Construct 1 / Construct 2) is represented on the bottom half of the trace, and the second half is represented on the top half of the trace. Steady state conductance values are noted to the right of each trace. Trace A represents the rectifying junction composed of ShakB N+16 and ShakB L tested by Phelan *et al* (2008). Trace B represents the SBL+N16NT-I19 paired with Shaking B lethal. Trace C represents coupling of the mutant SBL+N16NT with Shaking B lethal. Trace D represents the homotypic ShakB L/ShakB L junction tested by Phelan *et al* (2008). Trace E represents the Shaking B lethal/ Shaking B lethal junction tested in this study. Trace F represents the homotypic junction formed by ShakB N+16 paired with itself, tested by Phelan *et al* (2008). Trace G represents the mutant SBL+N16NT-I19 paired with itself. Trace H represents the mutant SBL+N16NT paired with itself. Figures from Phelan *et al.*, (2008) are reprinted from Curr. Biol. 18, Phelan, P., Goulding, L.A., Tam, J.L.Y., Allen, M.J., Dawber, R.J., Davies, J.A., and Bacon J.P., Molecular Mechanism of Rectification in the *Drosophila* Giant Fiber System. Pages No. 1955-1960. © (2007), With permission from Elsevier.



### *A Note Regarding Side-by-Side Comparison of Current Traces*

In several figures, current data is presented alongside current traces published in Phelan *et al.* 2008. These figures allow rapid visual comparison of the voltage-dependent gating characteristics of gap junction channels formed between paired oocytes. However, the experimental protocol of Phelan *et al.*, 2008 differed slightly from that used here. Phelan *et al.* (2008) used an eight step voltage pulse protocol compared to the ten-pulse protocol used in this study. A set of current traces recorded in our lab will therefore include four traces more than those of Phelan *et al.* (2008), representing currents induced by junctional voltages of  $\pm 90$  mV and  $\pm 100$  mV. In addition, the recordings of Phelan *et al.* (2008) were taken from oocyte pairs with lower conductance than pairs selected in this study. The conductance values are clearly marked next to each set of traces. Voltage-sensitivity is enhanced at lower conductance because a greater percentage of the voltage drop occurs across the junction (Wilders and Jongsma, 1982), we optimized voltage control across the junction by using electrodes containing silver chloride pellets rather than silver wires, and also by maintaining low resistance electrode tips (0.2 – 0.4 M $\Omega$ ). Hence, the differences are very slight as apparent in the comparison of wildtype ShalB L in the two studies.

### *Rectification of Electrical Synapses and Voltage Gating*

The biophysical nature of rectification in electrical synapses has been debated for decades (Jaslove and Brink, 1984, Goodenough and Paul, 2011). One possibility is that a rapid voltage-dependent gating mechanism favors channel opening when the presynaptic cell is depolarized. Another possibility is that asymmetric pairings create a pore that passes ions more easily in one

direction than another, an instantaneous rectifier. In this study the chimeric innexin, ShakBL N+16NT, formed a rectifying junction when paired with wildtype ShakBL. The properties of the junction were almost identical to those of ShakBL/ShakBN+16 heterotypic junctions suggesting the amino terminus is the domain responsible for creating rectification in heterotypic situations.

When paired with itself however, the chimera behaved like ShakBL. The homotypic junctions gated symmetrically, inactivating with a voltage-sensitivity and time-course similar to that of ShakBL. This suggests that gating due to transjunctional voltage ( $V_j$ ) involves domains other than the amino terminus. Hence rectification and  $V_j$ -dependent gating appear to be independent processes in ShakB. This does not rule out the possibility that rectification is dependent on voltage.

#### *Future Work*

The results observed in this study present a number of new questions that can be addressed. One of the first is the question of how the N-terminal replacement mutants would behave in a physiological system. It is now clear that these mutants are functional, and mimic the rectification effect, but how would the replacement of wildtype ShakB L in a fruit fly affect the escape response? This could further elucidate the role of the chemical synapses that co-occur with the rectifying synapses (Allen *et al.*, 2006).

The physiological significance of gap junction channel gating by factors such as voltage, pH and calcium are not well established. Since these mutations result in channels with altered properties, they could serve as a tool to better understand the significance of gating. In the future, such mutants will be used to create DNA construct amenable to insertion into the genome of *Drosophila melanogaster*. According to the protocol by Allen & Godenschwege (2010), the

mutant flies will then be subjected to electrophysiological testing *in vivo*. The flies will be anesthetized using carbon dioxide, or ice. The anesthetized fly will then be immobilized by pushing its legs, proboscis, and wings into dental wax. Five electrodes will be inserted into the fly. The grounding electrode will be inserted into the posterior end of the abdomen, while a stimulating electrode is inserted into each half of the brain by going through the eye. To ensure that the electrodes are in the proper brain region, short pulses will be given in order to cause movement of the wings. A recording electrode containing 3M KCl will then be inserted into the DLM of the fly, and a short pulse will be applied to the brain again to ensure proper insertion. Finally, this process of insertion into the muscle tissue will be repeated in the TTM on the side opposite the DLM insertion. A series of ten stimuli will then be induced with five seconds of resting time between stimuli. The response latency for each stimulus will be recorded, and the average taken. Then, a series of ten rapid fire stimuli will be induced with two seconds between the volleys of stimuli. This will be performed at frequencies of 100, 200, and 300 Hz. The number of responses will be compared against the number of stimuli given. The results of the mutants will be compared against the results obtained from wild type flies.

The escape response of the fruit fly is complex, involving multiple pathways. Motor neurons receive input from sources other than the rectifying synapses that are the focus of this study, hence it is of value to observe to what extent a mutation in the rectifiers will affect the speed at which the escape response occurs in the live organism. The role of the synapse between the TTMns and PSIs is not expected to play a role in this instance, because both the TTMns and PSIs most likely receive the same signal from the GFs, considering that each of these fibers are responsible for the actions of a separate muscle in the same reflexive response. The information gathered from *in vivo* experimentation can further elucidate the role of the rectifying electrical

synapse in the mixed synaptic region found at the Giant Fiber fork. The construction of the stimulation apparatus has been successful (Figure 28), and this work will soon be undertaken.

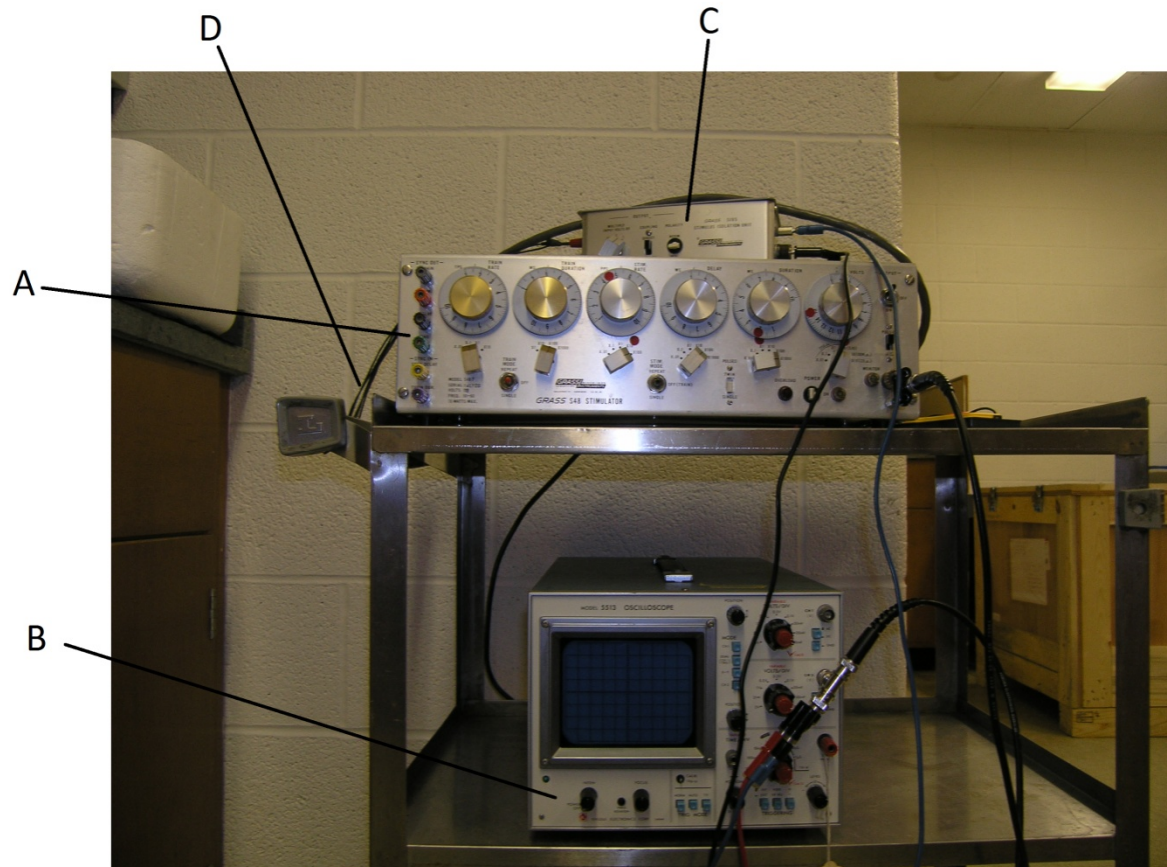


Figure 27

Figure 27. Photograph of the stimulation apparatus for use in electrophysiological testing of *Drosophila melanogaster*. The apparatus consists of several parts. A is the Stimulator. B is an oscilloscope for monitoring stimulus output. C is the stimulus isolation unit. D points to the wires into which the stimulus electrodes will be clipped.

In conjunction with the proposed *in vivo* study, further work can be performed on the junctions *in vitro*. Single channel recordings can provide a much clearer answer as to the way

the junctions rectify. A single channel recording would take the junctional conductance through one complete channel, and not the entire plaque. Observing the activity of one channel as opposed to hundreds can clarify exactly how sensitive these gap junctions are to voltage, and resolve the question of whether the rectification is indeed “instantaneous” in nature or if it is voltage dependent. Our lab is currently organizing a collaboration with others in the field who are well versed in this technique.

In addition to testing the mutant constructs in flies and performing single channel recording of the existing mutants, it would also be useful to test the mutants created in this study against wildtype ShakB N+16 to see what type of junction forms when the N termini are the same and the body of the protein differs. Also, switching the N-terminus of wildtype Shak B N+16 for that of Lethal, and testing those constructs against wildtype ShakB N+16 and against both wildtype ShakB L and the mutant constructs made in this study would be useful in further analyzing the role of the N-terminus in rectification. Testing mutations in both of the proteins involved in the rectification effect in the fruit fly GFS would give a richer understanding of the physiological role of the system, and would provide even more data to uncover the mechanism of rectification. This was the original goal of this study, however, unforeseen difficulties and delays led to the abandonment of Shak B N+16 mutagenesis.

Mutations can also be made in other domains of the ShakB proteins to discern what other parts may play a role in rectification. In connexins, it has been demonstrated that residues in the E1 domain involved in docking have an effect on rectification (Rubin *et al.*, 1992a). Additionally, the M3 domain has also been shown to have an effect (Rubin *et al.*, 1992b). The Shaking B proteins L and N+16 only differ up until midway through M2, after which point they share an identical sequence, eliminating the idea of M3 playing a role in this particular junction.

While M3 is likely not a factor, the E1 domains do differ from each other and it may be possible that part of the mechanism involves the binding of the different E1 domains. This study did not address that idea however, since all mutant were made from ShakB L in which the only alterations were made in the N-terminus.

In addition to the E1 domain, the gating polarity of the proteins may play a role in rectification in innexins. Oh, *et al.*, (1999 & 2000) demonstrated the effects of switching the gating polarity of this region of a connexin on rectification and channel polarity. Could switching the polarity of this region in an innexin have the same effect, or are innexins less influenced by interactions with the pore lining helices as shown by DePriest, *et al.*, (2011). Additionally, the “negative path” in the M1 of ShakB L may play a crucial role in rectification by acting in the voltage sensor apparatus. Perhaps altering this “negative” path can further clarify the mechanism of rectification. These are just a few of the potential directions this research could continue on in as the role of the innexin N-terminus is brought into focus.

## Works Cited

- Allen, M.J., Godenschwege, T.A., Tanoyue, M.A., Phelan, P. 2006. Making an escape: development and function of the *Drosophila* Giant Fiber System. *Sem. Cell Dev. Biol.* 17: 31-41
- Allen, M.J., Godenschwege, T.A. 2010. Electrophysiological Recordings from the *Drosophila* Giant Fiber System. *Cold Spring Harb Protoc.*: pdb.prot5453.
- Alexopoulos, H., Bottger, A., Fischer, S., Levin, A., Wolf, A., Fujisawa, T., Hayakawa, S., Gojoburi, T., Davies, J.A., Dvid, C.N., and Bacon, J.P. 2004. Evolution of Gap Junctions: The Missing Link? *Curr. Biol.* 14: R879-880.
- Auerbach, A.A. and Bennett, M.V.L. 1969. J. Gen. Physiol. A Rectifying Electronic Synapse In the Central Nervous System of a Vertebrate. 53(2): 211-237.
- Bear M., Connors B., and Paradiso M. 2007. Neuroscience: Exploring the Brain 3ed. Baltimore: Lippincott Williams & Wilkins. Pp.103-104.
- Brennan, M.A., DePriest, A.D., Karcz, J.A. Woolwine, Y. and Skerrett, I.M. (in prep). Tryptophan Scan of Cx32 Reveals Sites of Transmembrane Domain Interaction.
- Blagburn, J.M., H. Alexopoulos, J.A. Davies, and J.P. Bacon. 1999. Null mutation in *shaking-B* eliminates electrical, but not chemical, synapses in the *Drosophila* Giant Fiber System: A structural study. *J. Comp. Neurol.* 404:449-458.
- DePriest, A.D., Phelan, P., and Skerrett, I.M. (2011). Tryptophan scanning mutagenesis of the first transmembrane domain of the innexin Shaking-B(Lethal). *Biophys J.* 101: 2408-2416.
- Dong, L., Liu, X., Li, H., Vertel, B., and Ebihara, L. 2006. Role of the N-terminus in permeability of chicken connexin 45.6 gap junction channels. *J. Pysiol.*: 576.3:787-799.
- Furshpan, E.J., and Potter, D.D. 1959. Transmission at the Giant Motor Synapses of the Crayfish. *J. Physiol.* 145: 289-325.
- Goodenough, D.A., and D.L. Paul. 2009. Gap Junctions. *Cold Spring Harb. Perspect. Biol.* 1: a002576.
- Harris, A.L. 2001. Emerging issues of connexin channels: biophysics fills the gap. *Q. Rev. Biophys.* 34: 325-472.
- Holley, L.H. and Karplus, M. 1989 Protein secondary structure prediction with a neural network, *Proc. Natl. Acad. Sci.* 86: 152-156.

- Jaslove, S.W., and P.R. Brink. 1986. The mechanism of rectification at the electrotonic motor giant synapse of the crayfish. *Nature* 323:63-65.
- Karp G. 2008. Cell and Molecular Biology; Concepts and Experiments 5 ed. Hoboken: John Wiley & Sons. Pp.266-268.
- Kyle, J.W, Minogue, P.J., Thomas, B.C, Domowicz, D.A, Berthoud, V.M, Hanck, D.A, and Beyer E.C. An intact connexin N-terminus is required for function but not gap junction formation. *J Cell Sci.*121: 2744-2750
- Kyle, J.W., Berthoud, V.M., Kurutz, J., Minogue, P.J., Greenspan, M., Hanck, D.A., and Beyer E.C. 2009. The N terminus of connexin37 contains an  $\alpha$ -helix that is required for channel function. *J. Biol. Chem.*284: 20418–20427.
- Laird D.W. 2006. Life Cycle of Connexins in Health and Disease. *Biochem. J*; 394: 527-543.
- Leitch, B. 1992. Ultrastructure of electrical synapses: Review. *Electron Microsc. Rev.* 5: 311-339.
- Limon, A., Mauricio Reyes-Ruiz, J., Eusebi, F., and Miledi, R. 2007. Properties of GluR3 receptors tagged with GFP at the amino or carboxyl terminus. *Proc Natl Acad Sci U S A.* 104: 15526–15530
- Maeda S. Nakagawa S. Suga M. Yamashita E. Oshima A. Fujiyoshi I. Tuskihara T. Structure of the connexin 26 gap junction channel at 3.5Å<sup>o</sup> resolution. *Nature.* 2009;458: 597-607.
- Oh, S., Rubin, J.B., Bennett, M.V.L., Verselis, V.K., and Bargiello, T.A. 1999. Molecular determinants of electrical rectification of single channel conductance in gap junctions formed by connexins 26 and 32. *J. Gen. Physiol.*114: 339-364.
- Oh, S., Abrams, C.K., Verselis, V.K., and Bargiello, T.A. 2000. Stoichiometry of transjunctional voltage-gating polarity reversal by a negative charge substitution in the amino terminus of a connexin32 chimera. *J. Gen. Physiol.*116: 13-31.
- Oshima, A., Tani, K., Hiroaki, Y., Fujiyoshi, I., and Sosinsky, G.E. 2007. Three-dimensional structure of a human connexin26 gap junction channel reveals a plug in the vestibule. *Proc Natl. Acad. Sci (USA)*: 104: 10034-10039.
- Oshima, A., Tani, K., Kiroaki, Y., Fujiyoshi, Y., and Sosinsky G.E. 2008. Projection Structure of a N-terminal Deletion Mutant of Connexin 26 Channel with Decraesed Central Pore Density. *Cell Commun. Adhes.*: 15: 85-93.



- Peracchia, C (2004). Chemical gating of gap junction channels; roles of calcium, pH and calmodulin. *Biochim. Biophys. Acta.* 1662(1-2):61-80.
- Phelan, P., Nakagawa, M., Wilkin, M.B., Moffat K.G., O’Kane, C.J., Davies, J.A., and Bacon J.P. 1996. Mutations in Shaking-B Prevent Electrical Synapse Formation in the *Drosophila* Giant Fiber System. *J. Neurosci* 16: 1101-1113.
- Phelan, P., Stebbings, L.,A., Baines, R.,A., Bacon, J.P., Davies, J.A., and Ford C. 1998a *Drosophila* Shaking-B protein forms gap junctions in paired *Xenopus* oocytes. *Nature* 391:181- 184.
- Phelan. P, Bacon, J., Davies, J., Stebbings,. L., Todman, M., Avery, L., Baines, R., Barnes, T., Ford, C., Hekimi, S., Lee, R., Shaw, J., Starich, T., Curtin, K., Sun, Y., and Wyman, R. 1998b Innexins: a family of invertebrate gap-junction proteins. *Trends Genet.* 14: 348–349,
- Phelan, P., and T.A. Starich. 2001. Innexins get into the gap. *Bioessays* 23:388-396.
- Phelan, P., Goulding, L.A., Tam, J.L.Y., Allen, M.J., Dawber, R.J., Davies, J.A., and Bacon J.P. 2008. Molecular Mechanism of Rectification in the *Drosophila* Giant Fiber System. *Curr. Biol.*18: 1955-1960.
- Ringham, G.L. 1975. Localization and Electrical Characteristics of a Giant Synapse in the Spinal Cord of the Lamprey. *J. Physiol.* 251(2): 395-407
- Rubin, J.B., Verselis, V.K., Bennett, M.V.L., and Bargiello, T.A.1992a. Molecular analysis of voltage dependence of heterotypic gap junctions formed by connexins 26 and 32. *Biophys J.*62: 183-195.
- Rubin, J.B., Verselis, V.K., Bennett, M.V.L., and Bargiello, T.A., 1992b. A domain substitution procedure and its use to analyze voltage dependence of homotypic gap junctions formed by connexins 26 and 32. *Proc. Natl. Acad. Sci.*89: 3820-3824.
- Skerrett, I.M., Merrit, M., Zhou, L., Zhu, H., Cao, F., Smith, J.F., and Nicholson B.J. 2001. Applying the *Xenopus* oocyte expression system to the analysis of gap junction proteins. *Methods in Molecular Biology*154: 225-249.
- Verselis, V.K., Ginter, C.S., and Bargiello, T.A. 1994. Opposite voltage gating polarities of two closely related connexins. *Nature* 368: 348-351.
- Wang, J., and Dhal, G. 2010. SCAM analysis of Panx1 suggests a peculiar pore structure. *J. Gen. Physiol.* 136: 515-527.
- Wilders, R., and H.J. Jongsma. 1992. Limitations of the dual voltage clamp method in assaying conductance and kinetics of gap junction channels. *Biophys. J.* 63:942-953

- Willecke, K., Eiberger, J., Degen, J., Eckardt, D., Romualdi A., Guldenagel M., Urban, D., Goran, S. 2002. Structural and functional diversity of connexin genes in the mouse and human genome. *Biological Chemistry*. 383(5): 725-737.
- Yu, J., Bippes, C.A., Hand, G.H., Muller, D.J., and Sosinsky, G.E. 2007. Aminosulfonate modulated pH-induced conformational changes in connexin26 hemichannels. *J. Biol. Chem.* 282: 8895-8904.